

**NBS-GCR-80-251**

# **An Investigation of Fire Impingement on A Horizontal Ceiling**

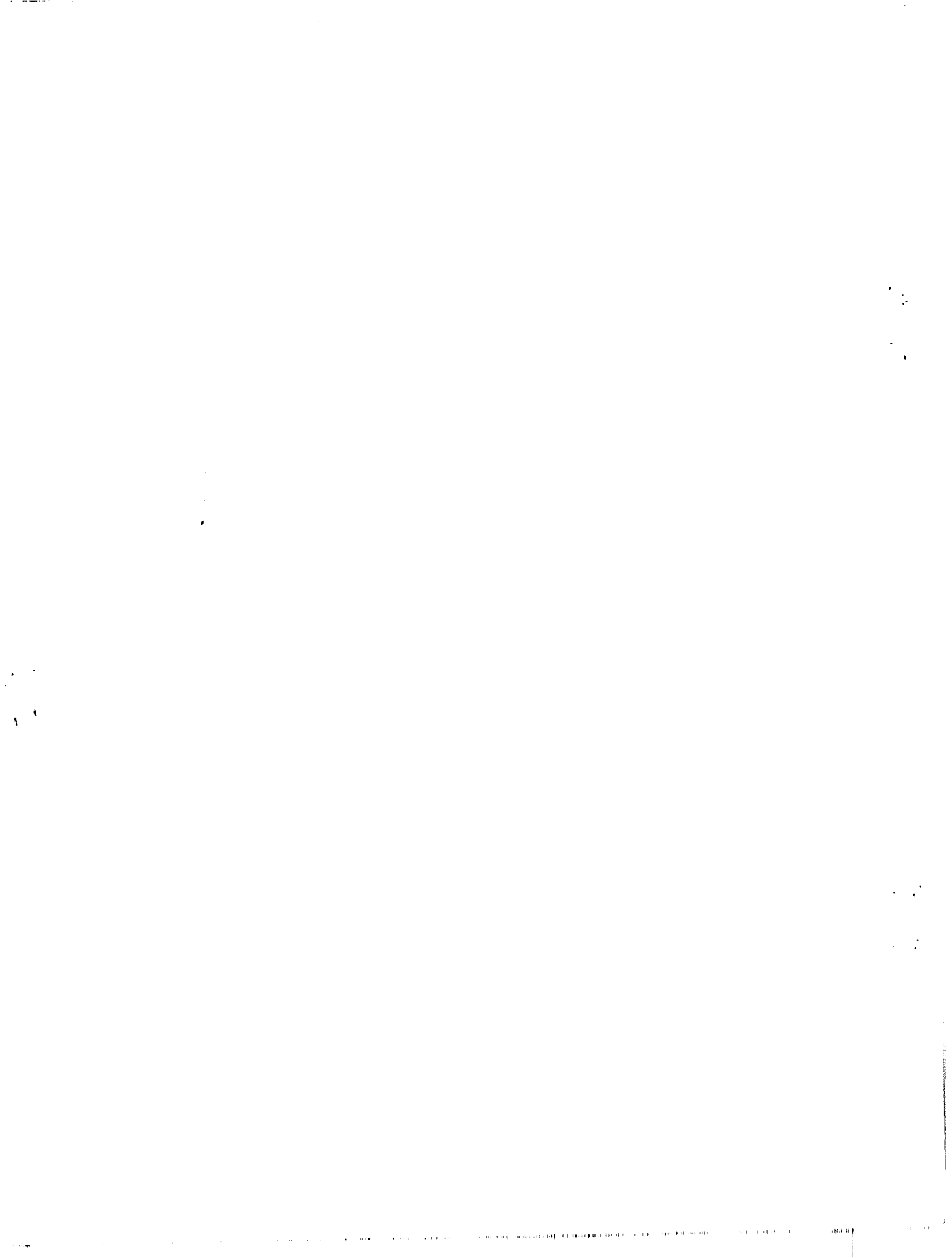
---

H-Z. You and G. M. Faeth

October 1979

Issued July 1980

Sponsored by  
**U.S. Department of Commerce  
National Bureau of Standards  
Washington, DC 20234**



NBS-GCR-80-251

**AN INVESTIGATION OF FIRE  
IMPINGEMENT ON A HORIZONTAL  
CEILING**

---

H-Z. You and G. M. Faeth

The Pennsylvania State University  
Department of Mechanical Engineering  
University Park, PA

October 1979

Issued July 1980

NBS Grant Number 7-9020

Sponsored by  
U.S. Department of Commerce  
National Bureau of Standards  
Washington, DC 20234



An Investigation of Fire Impingement  
on a Horizontal Ceiling

by

H-Z. You and G. M. Faeth

Department of Mechanical Engineering  
The Pennsylvania State University  
University Park, Pennsylvania

Prepared for

U. S. Department of Commerce

National Bureau of Standards  
Center for Fire Research  
Grant No. 7-9020

Dr. Howard Baum, NBS Scientific Officer

October 1979



### Notice

This report was prepared for the Center for Fire Research of the National Engineering Laboratory, National Bureau of Standards under Grant No. 7-9020. The statements and conclusions contained in this report are those of the authors and do not necessarily reflect the views of the National Bureau of Standards or the Center for Fire Research.



An Investigation of Fire Impingement  
on a Horizontal Ceiling

Summary

This report discusses research completed under NBS Grant No. 7-9020, during the period September 1, 1978 to August 31, 1979. The investigation considers the processes which occur when a turbulent fire impinges on a horizontal ceiling. The objectives of the study are:

1. Measure convective heat transfer rates to the ceiling.
2. Measure flame heights for impinging plumes and the radial extent of the flame under the ceiling for impinging fires.
3. Measure radiative heat fluxes to the ceiling and the ambience.
4. Measure flow structure for both impinging plumes and impinging fires, e.g. profiles of mean temperature, velocity and composition, as well as velocity fluctuations.

Experimental results are emphasized during the investigation although simplified theoretical models are considered to assist data correlation.

This report covers the second year of a three-year study. The first year of the investigation was devoted to convective ceiling heat flux measurements. The present effort concentrated on radiative heat flux measurements and a portion of the flow structure measurements.

A new experimental apparatus was constructed which allows the long term testing needed for structure measurements. This arrangement has a water-cooled ceiling, 1 m in diameter. The fire source is simulated by a 55 mm ID burner fueled with natural gas operating at heat release rates up to 8.5 kW. Convective and radiative heat fluxes are measured with heat flux gages, mean gas temperatures are obtained with fine wire thermocouples, mean velocities and velocity fluctuations are measured with a laser Doppler anemometer, an impact probe is also used for mean velocities, and mean concentrations are measured by isokinetic gas sampling and analysis with a gas chromatograph.

Measurements completed to date include: flame shape, convective and radiative heat fluxes to the ceiling, radiative heat fluxes to the ambience, mean temperatures, and mean velocities and velocity fluctuations in the plume portion of the flow.

The results, thus far, can be summarized as follows:

1. Convective heat fluxes to the ceiling can be correlated by the following expression:

$$(\dot{q}'' H^2 / \dot{Q}) Ra^{1/6} Pr^{3/5} = 31.2 \quad r/H < 0.16 \quad (I)$$

$$= 1.46(r/H)^{-1.63} \quad r/H < 0.16 \quad (II)$$

for the range  $10^9 < Ra < 10^{14}$ ,  $H_f/H < 1.5$ ,  $Pr \approx 0.7$ . Larger flame heights result in reduced heat fluxes in the stagnation region,  $r/H < 0.16$ , while laminar impinging flows yield higher heat fluxes than Eq. (I). Both these effects are less important in the ceiling

jet region,  $r/H < 0.16$ . The correlations are limited to unconfined ceilings. Results from the first phase of this study suggest that heat fluxes are somewhat higher for confined ceilings, although Eqs. (I) and (II) provide a reasonable first estimate.

2. The maximum flame radius in the plume occasionally reaches  $r/z = 0.4$ , which corresponds to the full width of the thermal boundary layer. Similar behavior is observed in the flaming portion of the ceiling jet.
3. The plume portion of the flame exhibited the three zone structure delineated by McCaffrey [12]. This includes a region of increasing temperatures and velocities near the source; a region where temperatures and velocities vary relatively slowly near the tip of the flame, and a region of declining temperatures and velocities in the non-combusting portion of the flow. In the latter region,  $z/\dot{Q}^{2/5} > 0.2 \text{mkW}^{-2/5}$ , mean temperature and velocities along the axis of flow could be correlated as follows

$$T_c - T_\infty = 11(g\beta\rho^2 C_p^2)^{-1/3} (z/\dot{Q}^{2/5})^{-5/3} \quad (\text{III})$$

$$w_c/\dot{Q}^{1/5} = 3.4(g\beta/\rho C_p)^{1/3} (z/\dot{Q}^{2/5})^{-1/3} \quad (\text{IV})$$

where properties in these expressions are taken as local ambient properties. Equation (III) corresponds to the correlation of Rouse, et al. [19] while Eq. (IV) corresponds to the recommendation of George, et al. [20]. Other correlations in the literature, as well as the recent measurements of McCaffrey [12] and Cox and Chitty [13], exhibit similar trends with distance but somewhat different magnitudes. We also find differences in flow widths from earlier results. These discrepancies could be the result of scale effects, further study is needed to resolve these differences - even for the well-studied plume region.

The measurements reported here also show differences from those of Refs. 12 and 13 in the near source and flame tip regions. These regions are more dominated by source characteristics and this behavior is to be expected. Clearly, a more general theory than now exists will be required to predict behavior in these regions.

4. Mean temperatures are reported for the ceiling jet region. The presence of flames results in a thicker boundary layer. Reynolds number effects are also observed. The temperature profile at the wall becomes steeper with increasing distance from the stagnation point. Similar development effects were observed during an earlier study of wall plumes in this laboratory.

Measurements of mean velocities in the ceiling jet and composition throughout the flow are in progress. Subsequent tests will also consider larger scale systems, since the results to date suggest important effects of fire size on turbulence and mixing characteristics.

Acknowledgement

This research was supported by the United States Department of Commerce, National Bureau of Standards, Grant No. 7-9020. Dr. Howard Baum of the Center for Fire Research was the NBS Scientific Officer for the Project.

Table of Contents

	<u>Page</u>
Summary . . . . .	ii
Acknowledgement . . . . .	iv
List of Tables . . . . .	vi
List of Figures . . . . .	vii
Nomenclature . . . . .	viii
<u>1. Introduction</u> . . . . .	1
<u>2. Experimental Apparatus</u> . . . . .	2
2.1 Apparatus . . . . .	2
2.2 Instrumentation . . . . .	4
<u>3. Theory</u> . . . . .	13
<u>4. Results and Discussion</u> . . . . .	13
4.1 Ceiling Heat Fluxes . . . . .	13
4.2 Flow Structure . . . . .	20
4.2.1 Flame Shape . . . . .	20
4.2.2 Mean Temperatures . . . . .	20
4.2.3 Mean and Fluctuating Velocities . . . . .	25
4.2.4 Radiation Measurements . . . . .	35
References . . . . .	36

List of Tables

<u>Table</u>	<u>Title</u>	<u>Page</u>
1	Composition of Fuel Gas . . . . .	5
2	Summary of Instrumentation. . . . .	6
3	Laser Doppler Anemometer Measuring Volume . . . . .	12
4	Theoretical Models and Correlations under Consideration .	14
5	Test Conditions for Ceiling Heat Flux Measurements. . . .	15
6	Plume Profile Constants . . . . .	26

List of Figures

<u>Figure</u>		<u>Page</u>
1	Sketch of the experimental apparatus . . . . .	3
2	• Details of ceiling instrumentation . . . . .	9
3	Sketch of the laser Doppler anemometer system. . . . .	10
4	Convective and total heat flux at the ceiling stagnation point . . . . .	17
5	Radial variation of convective heat flux to the ceiling. . . . .	18
6	Correlation of convective heat flux to the ceiling. . . . .	19
7	Flame shape, 1.67 kW fire (condition 7). . . . .	21
8	Flame shape, 8.41 kW fire (condition 8). . . . .	22
9	Mean temperature variation along the flame axis. . . . .	24
10	Radial mean temperature profiles, 1.67 kW fire (condition 7) . . . . .	27
11	Radial mean temperature profiles, 8.41 kW fire (condition 8) . . . . .	28
12	Mean temperature profiles in the ceiling jet, 1.67 kW fire (condition 7) . . . . .	29
13	Mean temperature profiles in the ceiling jet, 8.41 kW fire (condition 8) . . . . .	30
14	Mean velocity measurements using the LDA in a buoyant plume. . . . .	32
15	Longitudinal velocity fluctuations in a buoyant plume. . . . .	33
16	Mean velocity variation along the flame axis . . . . .	34

Nomenclature

<u>Symbol</u>	<u>Description</u>
$C_p$	specific heat
$C_T$	plume parameter, Eq. (3)
$C_w$	plume parameter, Eq. (2)
$f$	friction factor
$g$	acceleration of gravity
$H$	ceiling height
$H_f$	free flame height
$H_R$	radial extent of flame along ceiling
$Pr$	Prandtl number
$\dot{q}''$	ceiling heat flux
$\dot{Q}$	plume thermal energy flux
$r$	radial distance
$Ra$	Rayleigh number - $g\beta\dot{Q}H^2/\rho C_p \nu^3$
$T$	temperature
$w$	vertical velocity
$W$	plume buoyancy flux
$z$	height above source
$\beta$	coefficient of thermal expansion
$\nu$	kinematic viscosity
$\rho$	density

Subscripts

$c$	centerline of plume
$\infty$	ambient condition



## 1. Introduction

In order to gain a better understanding of fires within structures, several comprehensive fire models have recently been developed [1-5].\* These models are constructed by combining specific models of subprocesses within the fire environment. The development of this approach has motivated the need for additional information on fire subprocesses.

The present investigation is concerned with one of these subprocesses; namely, the impingement of fires and fire plumes on a ceiling. The objective of the research is to study radiative and convective heat transfer rates between the flow and the ceiling as well as the structure of the flow. Simplified theoretical models are also being considered, in order to provide a means of data correlation so that the present results can be utilized by comprehensive models.

The phenomena of a fire or fire plume striking a ceiling is clearly an important aspect of fires within structures. Therefore, the problem has attracted the attention of a number of earlier investigators [6-11]. Three regions of the flow have been distinguished: the plume, prior to impingement; the stagnation region, corresponding to  $r/H < 0.2$  [10]; and the ceiling jet region, corresponding to  $r/H > 0.2$ . The characteristics of the flow are also influenced by the degree of confinement of the ceiling (since a stratified ceiling layer forms under the ceiling when it is confined) and by the extent which flames strike the ceiling.

Previous studies of impingement on ceilings have been primarily concerned with the ceiling jet region, for plume impingement on an unconfined ceiling. Alpert [9, 10] has developed an integral model describing this flow. Predictions of convection heat transfer rates, using this model, compared reasonably well with measurement. Zukoski, et al. [11], confirm these findings in a later study. Radiative effects, flame impingement, the stagnation region, and the structure of the flow (velocities, temperatures, concentrations and turbulence quantities), however, have not received much attention in the past.

Plumes and fire plumes have been the subject of numerous investigations; e.g., Refs. 12-22, to name only a few. In spite of this effort, there have been very few studies of the flame structure above natural fires. The recent measurements of mean temperatures and velocities by McCaffrey [12] and Cox and Chitty [13] are a notable exception. This state of affairs is unfortunate since the plume provides the initial condition for the impingement problem.

With this status in mind, the present study considers fire and fire plume impingement on a ceiling with the following specific objectives:

1. Measure convective heat transfer rates to the ceiling.
2. Measure flame heights for impinging plumes and the radial extent of the flame under the ceiling for impinging fires, in order to define the regions of the flow where combustion must be considered.

---

\*Numbers in brackets denote references.

3. Measure radiative heat fluxes to the ceiling and the ambience.
4. Measure the structure of the flow for cases involving both impinging plumes and fires. The structure measurements include profiles of mean temperature, velocity and composition, as well as velocity fluctuations.

The investigation emphasizes experimental results. The use of theory is confined to simplified models as an aid to data correlation.

The first year of the investigation concentrated on items 1 and 2. The results of this effort are reported in Refs. 23-25. Fire sources were simulated by burning wicks soaked with liquid methanol, ethanol, 1-propanol and n-pentane. Ceiling heat fluxes were obtained by measuring the rate of temperature rise of a copper ceiling. Correlations were obtained for free flame heights, the radial extent of impinging flames along the ceiling, the ceiling heat flux in the stagnation region, and the ceiling heat flux in the ceiling jet region. Confined and unconfined ceilings were considered for both fire plume and fire impingement. The new results were in good agreement with earlier work [9-11], for the case of plume impingement on an unconfined ceiling.

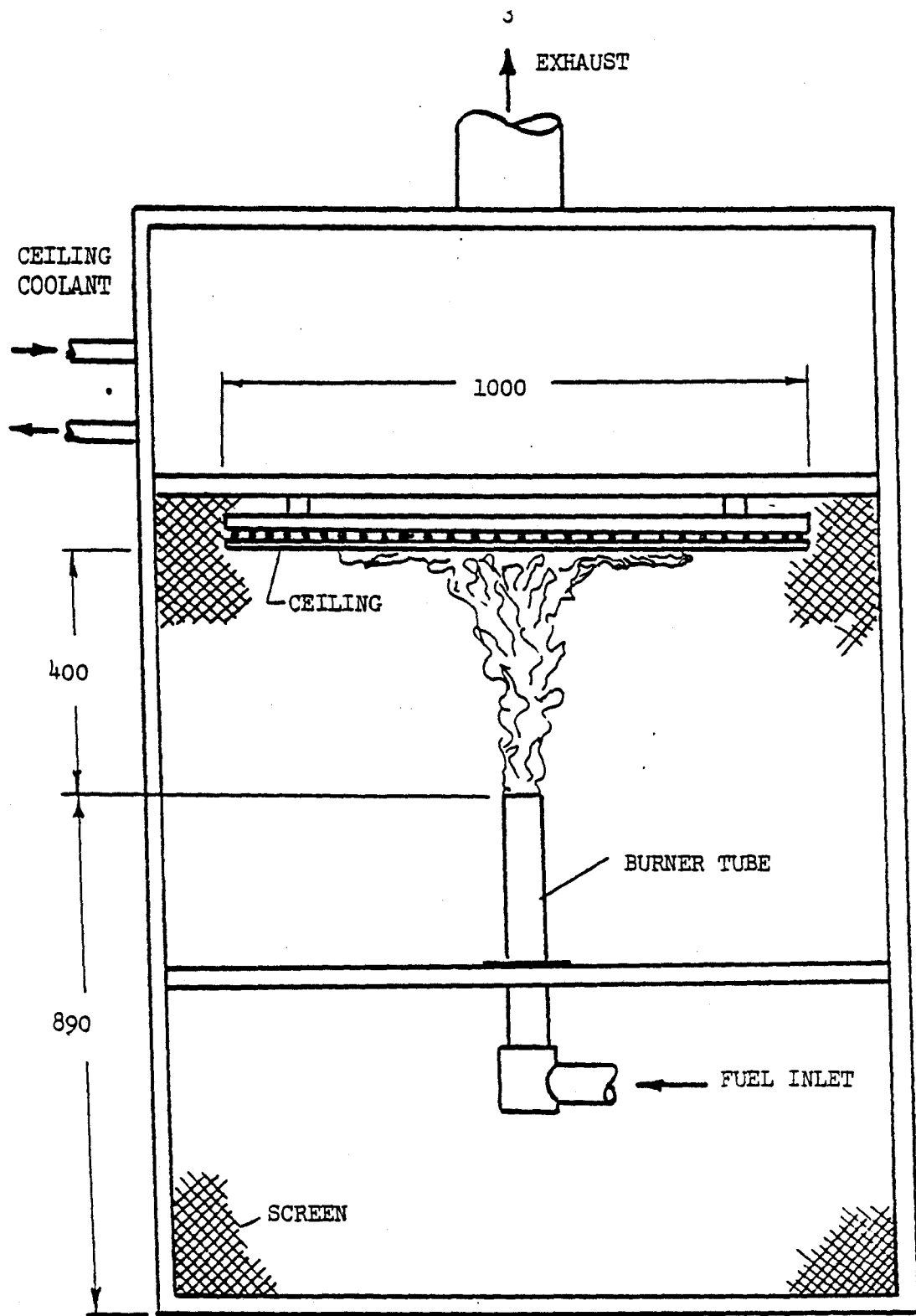
This report considers activities during the second year of study when items 3 and 4 were emphasized. The main objective of this work was to develop a new apparatus which provides the long term testing capabilities needed for structure measurements. This apparatus has been employed to obtain new data on radiative and convective heat fluxes to the ceiling, radiative heat fluxes to the ambience and flame shapes. A portion of the flow structure measurements was also completed, specifically, mean temperatures and velocities and turbulence quantities. The remaining measurements are in progress and will be reported in the near future.

## 2. Experimental Apparatus

### 2.1 Apparatus

A sketch of the experimental apparatus is illustrated in Fig. 1. The main components of the apparatus are a fire source, a cooled ceiling and an exhaust system. Drafts can significantly influence plume characteristics. Therefore, the tests are conducted in an interior room having dimensions 4 m x 6 m and a ceiling height of 5 m. The flow is further protected from disturbances by using the screened enclosure illustrated in Fig. 1. This involves a single layer of screen (630 wires per m, square pattern, 0.25 mm wire diameter). The top of the apparatus acts as a gas collector for a natural draft exhaust system.

No floor is provided at the level of the fire source. Eliminating the floor improves access to the flame and helps to steady it in the presence of room disturbances. The absence of a floor has not been found to influence natural fires to a great degree [13].



DIMENSIONS IN MM

Fig. 1 Sketch of the experimental apparatus.

The fire source is simulated by a natural gas fueled diffusion flame. The natural gas at this location is largely methane. The nominal fuel composition is summarized in Table 1. The gas flow rate is controlled with a set of valves providing course and fine adjustment. The gas flow rate is measured with a rotameter, which was calibrated with a wet-test meter.

The burner tube used for most of the tests is a stainless steel cylinder with an inside diameter of 55 mm. Stainless steel wool packing and an array of fine mesh screens (screens 45 mm apart, 3940 wires per m, square pattern, 0.66 mm wire diameter) in the vertical portion of the burner provides a uniform velocity profile at the exit. A single screen, having similar characteristics, is spot-welded across the exit of the tube in order to prevent flame attachment within the tube, at low gas flow rates.

Some measurements of ceiling heat fluxes employed a premixed flame source. The objective of these tests was to separate effects due to active combustion in a diffusion flame, from effects normally encountered in a heated plume. The premixed burner had a 25 mm I.D. exit port but was otherwise similar to the larger port used during the diffusion flame experiments.

The cooled ceiling has a diameter of 1000 mm. The ceiling is constructed of a 12.7 mm thick aluminum disk. The lower surface of the disk is coated with a radiation absorbing paint (3M Nextel 101 C-10) having an emissivity of 0.96.

The ceiling is cooled from its upper surface with a spiral wound coil (4 parallel flow circuits, 2.5 mm OD x 0.9 mm wall thickness copper tubing, with coils spaced 51 mm apart). The cooling coils are bonded to the ceiling using Devcon F putty. The ceiling is insulated from above with a 50 mm thick layer of Fiberfrax Lo-Con Blanket (Carborundum Company), coated with aluminum foil.

The water coolant is recirculated from a large drum within the test area. This arrangement is described in an earlier report [26]. By controlling the flow of makeup water to the drum, the ceiling can be maintained within a few degrees of the ambient temperature at all operating conditions. The combination of coolant passage spacing and ceiling thickness also limits ceiling temperature variations to within a few degrees, even with impinging flames.

## 2.2 Instrumentation

The instrumentation can be divided into three groups: monitoring, ceiling measurements and profile measurements. The instrumentation used in each group is summarized in Table 2.

Monitoring Instrumentation. The monitoring instrumentation is not particularly unusual. The temperatures are indicated with a Hewlett-Packard, Model 2401C integrating digital voltmeter. Two different sized rotameters are used to monitor the fuel gas flow rate, due to the large flow rate range used in testing.

TABLE 1

Composition of Fuel Gas

Species	Percent by Volume
Methane	94.863
Ethane	3.753
Propane	0.266
iso-Butane	0.039
n-Butane	0.047
iso-Pentane	0.019
mono-Sulfur	0.009
di-Sulfur	0.012
Mercaptans	0.016
n-Pentane	0.016
Hexane	0.084
Nitrogen	0.408
Carbon Dioxide	0.423
neo-Pentane	0.006
Hydrogen Sulfide	0.019
Hydrogen	0.020

TABLE 2

Summary of Instrumentation

Function	Instrument	Number Required
Monitoring:		
Coolant Flow Rate	Rotameter	1
Coolant inlet and outlet temperatures	Chromel-alumel thermocouple - stainless steel sheath, 3.2 mm O.D., 65 mm immersion length	2
Ceiling temperatures	Chromel-alumel thermocouple bare wire, 0.8 mm O.D., welded junction cemented to top side of wall, under insulation -	6
Fuel gas flow rate	Rotameters, high and low range for conditions 1 and 2, and 3 and 4	2
Burner tube temperature	Chromel-alumel thermocouple, bare wire, 0.8 mm O.D., spot-welded to burner	2
Ambient temperature	Chromel-alumel thermocouple bare wire, 0.8 mm O.D. at ceiling and burner heights	2
Ambient pressure	laboratory, mercury barometer	1
Ceiling Measurements:		
Heat fluxes	Foil-type heat flux gage HyCal, Model LO-4 gold foil surface for convection only, black foil surface for total heat flux	11 positions
Static pressures	1.2 mm O.D. static pressure taps and electronic manometer	9 positions
Profile Measurements:		
Mean velocities and turbulence quantities	Helium-neon LDA, dual-beam forward scatter, frequency shifted	1
Mean velocities	Impact-static probe, 1.5 mm O.D. probe tip, 2 mm O.D., quartz tube and electronic manometer	1
Composition	Quartz microprobe, 0.4 mm O.D. probe tip, 2 mm O.D., sonic quenching and gas chromatograph for CH <sub>4</sub> , C <sub>2</sub> H <sub>6</sub> , H <sub>2</sub> , CO <sub>2</sub> , CO, H <sub>2</sub> O, O <sub>2</sub> and N <sub>2</sub>	1

(continued)

Function	Instrument	Number Required
Temperature	Pt/Pt - 10% Rh bare wire thermocouple, .076 mm O.D. wires	1
Radiative heat flux	Medtherm Radiation Heat Flux Transducer, Type 64F-10-22 150 degree viewing angle, mounted on probe just outside edge of flow.	1
Flame shape	Graphlex, 4 x 5 still camera 2000 ASA Polaroid film, probe visual observation.	1

Ceiling Measurements. Radiative and convective heat fluxes, and static pressures are measured along the ceiling. The arrangement of this instrumentation is illustrated in Fig. 2.

The heat flux gage at the center of the ceiling is surrounded by a cooling passage. The remainder of the gages are centered under cooling passages as illustrated in Fig. 2. The lower surface of the gage is flush with the surface of the ceiling. This surface is coated with either gold foil, for a convective heat flux measurement, or with a black coated foil (3N Nextel 101 C-10), for a total heat flux measurement. The radiative heat flux to the ceiling is obtained by taking the difference between these two measurements. Good thermal contact was provided between the heat flux gages and adjacent surfaces coating contact areas with a silicon heat sink (type 340) compounded by Dow Corning.

Problems were encountered with the gold foil becoming tarnished with soot, particularly at positions near the center of the ceiling. This necessitated frequent replacement of gold foils. In some cases, it was necessary to protect the gage surface with an insulated pad, which was removed for a measurement after the system had stabilized.

The static pressure taps in the ceiling are of typical design. The tubing connecting the taps to the pressure transducer is arranged so that all tubes have the same thermal path. This is necessary since the static pressure differences are small and can be affected by hydrostatic pressure differences due to heated sections of tubing. The pressure is measured with a CGS Datametrix Model 1014 A electronic manometer, which employs a Model 1056 null offset adapter and a Model 570D-10T02A1-V1, 0-10 Torr differential pressure transducer.

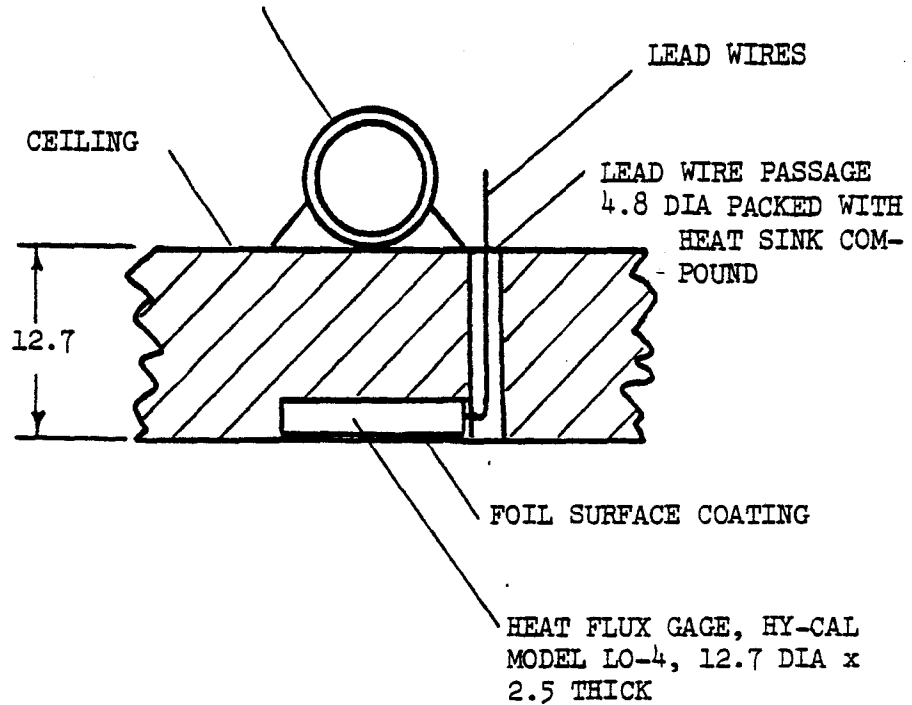
Structure Measurements. The structure measurements involve mean and fluctuating velocities, mean temperatures, mean compositions, radiant heat flux, and flame shape.

The laser Doppler anemometer (LDA) is the basic instrument used for measuring mean velocities and turbulence quantities. A sketch of this arrangement appears in Fig. 3. A dual-beam forward-scatter arrangement is used with a Bragg cell frequency shifter so that flow reversals can be detected and accurate results can be obtained near the edge of the flow. The system includes a 50 mW helium-neon laser, Spectra Physics Model 125A, and the following Thermo-Systems Inc. equipment: Model 1090-1 tracker system, Model 980-2 frequency shifter, Model 910-2 transmitting optics, Model 930 receiving optics, Model 960 photomultiplier system and Model 1060 true R.M.S. meter. The output signal from the detector is monitored with an oscilloscope. Averages are obtained in the turbulent flow using a Hewlett-Packard Model 2401C integrating digital voltmeter.

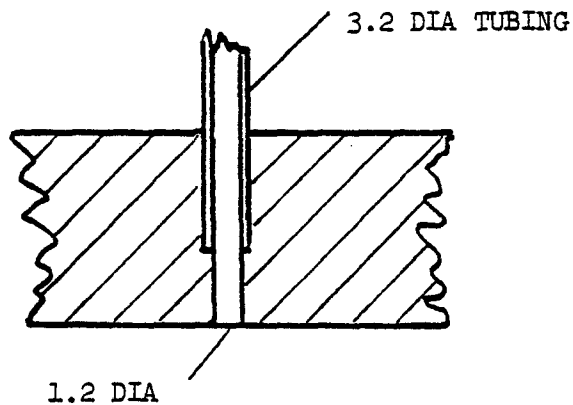
The LDA actually measures the velocity of small seeding particles (less than 1  $\mu\text{m}$  in diameter) in the flow. Obtaining proper seeding levels proved to be one of the more difficult problems during the tests. In the upper regions of the flames, sufficient soot is formed so that seeding levels are reasonably adequate. It was necessary to supplement this natural source of particles with small condensed oil drops near the edge of the flow. The oil particle generator used for this purpose yields particles densities of  $2.8 \times 10^{10}$  particles/ $\text{m}^3$  with an average particle diameter of 0.6  $\mu\text{m}$  [27]. Finally,

ALL DIMENSIONS IN MM

COOLANT PASSAGE 9.5 DIA



DETAIL OF HEAT FLUX GAGE INSTALLATION



STATIC PRESSURE TAP INSTALLATION

Fig. 2 Details of ceiling instrumentation.

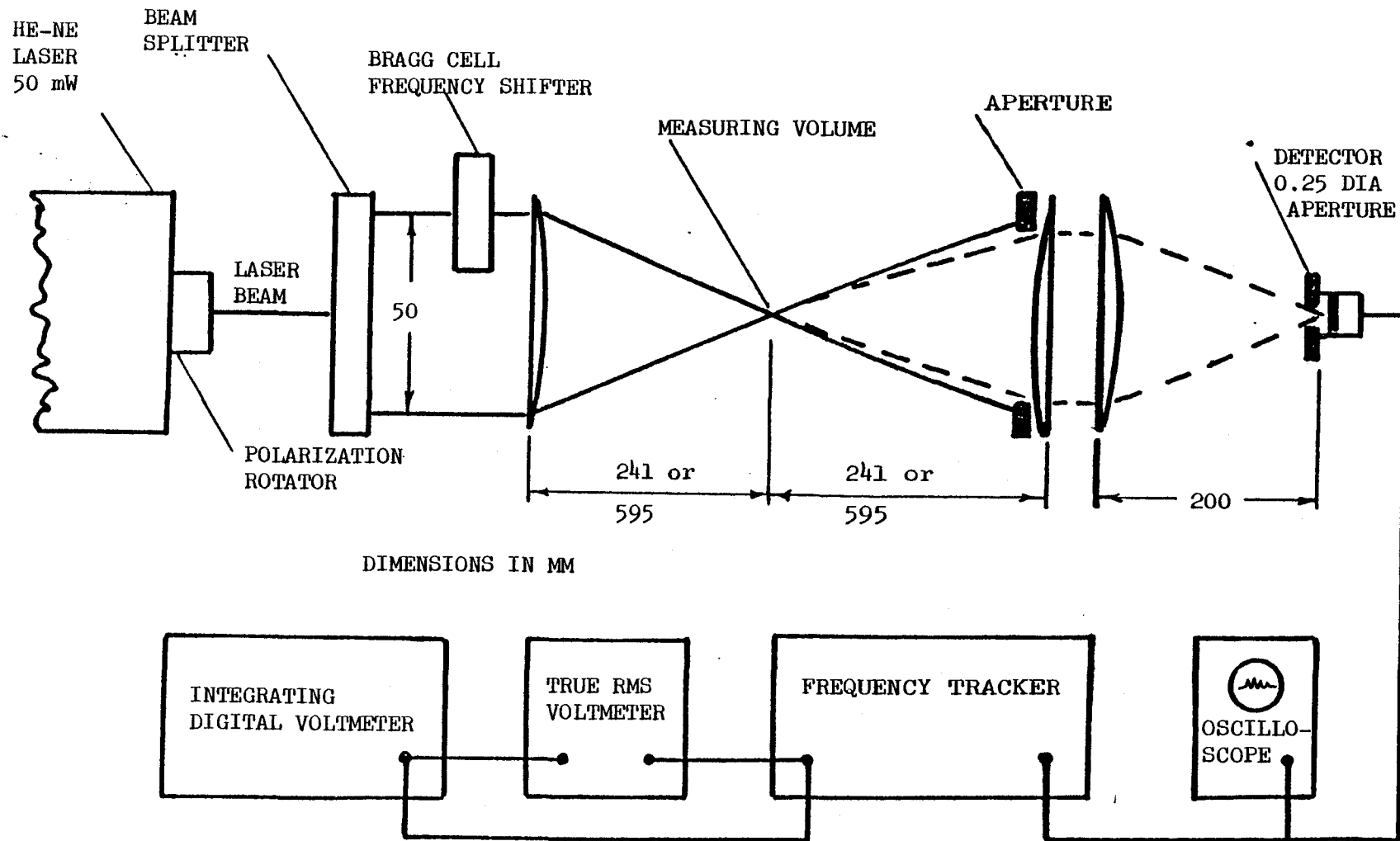


Fig. 3 Sketch of the laser Doppler anemometer system.

particle densities in the lower portions of the flame were increased by adding a small flow of acetylene to the fuel gas. Overall, all particles are sufficiently small so that they represent the flow velocities reasonably well, yielding a flat frequency response to 7 kHz.

The LDA system illustrated in Fig. 3 employs two different optical systems, having different focal lengths for the sending and receiving optics. The dimensions of the measuring volume for these two arrangements are summarized in Table 3. The shorter focal length arrangement must be used in the lower portion of the plume. The longer focal length system is used in the impingement region since the experiment must fit between the lenses and the larger measuring volume reduces seeding requirements.

The frequency tracker provides a signal proportional to the instantaneous flow velocity in the measuring volume. This signal can be processed similar to a hot-wire signal. Mean velocities are found by integrating the signal, fluctuating velocities are found with the true RMS meter. Various velocity components and the Reynolds stress can be found by rotating the plane of the laser beams [28].

The use of the LDA proved to be very difficult in the ceiling jet region. The path lengths of the laser beams are quite long, through a turbulent variable density flow, which disturbs the fringe pattern at the measuring volume. It was also difficult to maintain adequate rigidity of the system while attempting to move the heavy ceiling in order to obtain profile measurements. Therefore, an impact-static probe is used for velocity measurements in the ceiling jet region. This probe is similar to the arrangement used during an earlier wall plume study in this laboratory [29]. In this case, the static probe provides a means of compensating for hydrostatic pressures variations both at the measuring location and in the thermal path of the tubing. These pressures are measured in the same manner as the static pressure measurements along the ceiling.

The composition of gaseous species is measured by sampling and analysis using a gas chromatograph. In order to provide good spatial resolution, a quartz microprobe (tip diameter 0.4 mm) is used for sampling. The samples are analyzed for methane, ethane, hydrogen, carbon dioxide, carbon monoxide, water vapor, oxygen and hydrogen with a Varian Model 3720 gas chromatograph employing a hot wire detector. The chromatograph is calibrated with samples prepared by the Scott Company

Gas temperatures are measured with a fine-wire (0.075 mm O.D. wires and junction) thermocouple constructed of Pt/Pt-10% RH. This thermocouple is about six times larger than the unit employed during the wall plume study. This change was made due to the excessively short lifetime of the smaller junction when used in the combusting portions of the flow. The radiation correction for the present junction is still relatively low (on the order of 20 C at the flame tip). Corrections for radiation errors are made for each point in the flow since velocities and compositions are known. Mean temperatures are obtained by integrating the signal with the integrating digital voltmeter.

TABLE 3

Laser Doppler Anemometer Measuring Volume<sup>a</sup>

Focal Length of Transmitting and Receiving Optics (mm)	Measuring Volume Dimensions (mm) <sup>b</sup>	
	Minor Diameter	Major Diameter
241	0.14	1.4
595	0.34	8.2

<sup>a</sup>Beam diameter 1.8 mm. Aperture diameter 0.25 mm. Helium-neon laser, wavelength 632.8 nm.

<sup>b</sup>The minor diameter is normal to the optical axes, the major diameter is parallel to the optical axis.

Radiant heat flux from the flow to the ambience is also measured. The radiation sensor is a probe-mounted, gas-purged, water-cooled sensor (Medtherm Radiation Heat Flux Transducer, Type 64F-10-22, 150 degree viewing angle). The sensor is mounted close to the edge of the ceiling layer, with its face parallel to the ceiling. The sensor readings are corrected for the 150 degree view angle, the effect of optically thick and thin flames (as limits), following the procedure outlined by Orloff, et al. [30]. The sensor output is measured with an integrating digital voltmeter.

The final measurement made on the test flames is flame shape, defined as the visual edge of the flame. Two methods have been employed for this measurement. The first method involves photographing the flame with a still camera in a darkened room. A series of photographs are taken normal to the axis of the flame, and for impinging flames, normal to the axis of the ceiling. These photographs are then measured to yield the maximum, minimum and average flame position as a function of distance from the burner.

Photographs are subject to error since they are a two-dimensional view of a three-dimensional phenomena, and are influenced by time of exposure, developing techniques, and the subjective judgement of the position of the flame boundary on the film. Therefore, direct observation of the flame is also employed. This involves positioning a probe at the maximum and minimum flame positions for a range of axial distances from the burner, similar to earlier work [23-25].

### 3. Theory

Theoretical activities are confined to consideration of existing models of various plume impingement processes and the examination of simplified correlations which can summarize results in a form that can be employed in comprehensive fire models.

The models being considered are summarized in Table 4. A number of processes are considered - several models are available for most of them. In the case of impinging combustions, only a limited number of empirical correlations are available for comparison with each measurement, all of which were found during the first phase of the present study [23-25].

### 4. Results and Discussion

Measurements of ceiling heat fluxes, radiant heat fluxes, flame shape and mean temperatures have been completed. A portion of the velocity and velocity fluctuation measurements have also been completed. A representative sample of these results will be presented and discussed in the following. The remainder of the measurements and a more complete analysis of the data are currently in progress and will be reported in the near future.

#### 4.1 Ceiling Heat Fluxes

Table 5 is a summary of the test conditions employed for the ceiling heat flux measurements. During the experiments, complications were encountered

TABLE 4

## Theoretical Models and Correlations under Consideration

Process	Source
Plume structure prior to impingement	Rouse, et al. [19] George, et al. [20] Yokoi [21] Emmons, et al. [1]
Flame length and structure prior to impingement	Steward [17] Wilcox [18] Cox and Chitty [13] McCaffrey [12]
Flame length after impingement	You and Faeth [23-25]
Noncombusting stagnation region convective heat fluxes	You and Faeth [23-25] Donaldson, et al. [31]
Noncombusting ceiling jet convective heat fluxes	Alpert [9,10] You and Faeth [23-25] Emmons, et al. [1]
Combusting stagnation region convective heat fluxes	You and Faeth [23-25]
Combusting ceiling jet convective heat fluxes	You and Faeth [23-25]
Noncombusting ceiling jet structure	Alpert [9,10]

Table 5  
 Test Conditions for Ceiling Heat Flux Measurements<sup>a</sup>

Condition	Q(W)	H(mm)	Ra x 10 <sup>12</sup> <sup>b</sup> H <sub>f</sub> /H		Data Symbol
<u>Premixed Flame, 25 mm ID burner port</u>					
1	240	480	0.38	0.10	□
2	240	635	0.70	0.08	◻
3	385	480	0.64	0.20	○
4	385	635	1.11	0.15	◌
5	709	480	1.16	0.41	△
6	709	635	2.05	0.24	△
<u>Diffusion flame, 55 mm ID burner port</u>					
7	1670	410	1.97	1.00	◌
8	8410	410	10.00H <sub>R</sub> /H=0.56		◻

<sup>a</sup>Ambient conditions air, 294-300k, 97-99kPa

<sup>b</sup>Evaluated using the following properties:  $\rho = 1.117 \text{ kg/m}^3$ ,  $g = 9.806 \text{ m/s}^2$ ,  
 $C_p = 1.005 \text{ kJ/kgK}$ ,  $\nu = 15.7 \times 10^{-6} \text{ m}^2/\text{s}$ ,  $Pr = 0.70$

concerning effects of flow development, and the degree of completion of oxidation of the fuel. In order to help separate these phenomena, both premixed flames (with relatively short flame heights) and diffusion flames (which involve flame impingement on the ceiling) were considered in the experiments.

Figure 4 is an illustration of convective and total heat fluxes at the ceiling stagnation point. In addition to the present data, the earlier results obtained during this study, and a correlation based on theoretical analysis of the stagnation region, are also illustrated [23-25]. The convective and the total ceiling heat fluxes are distinguished by the shading of the symbols for the present data. The earlier results had relatively small radiative effects [23-25].

The new measurements are in reasonably good agreement with the earlier results and the correlation. Even though the present measurements were obtained for stable operating conditions, the degree of apparent scatter is similar to the earlier results. Two factors are responsible for this. If the flow is not fully developed, the plume exhibits laminar-like tendencies, resulting in higher heat fluxes at the stagnation point. This is due to the fact that laminar plumes mix more slowly with the ambience than turbulent plumes, preserving higher plume velocities and temperatures near the centerline. Therefore, the more fully developed flows tend to give lower heat fluxes at a given condition. The second factor involves the effect of combustion. In cases where the flame spreads a significant distance along the ceiling, the core of the flame begins to contact the stagnation point. The low velocities and temperatures in this core region result in a reduction in stagnation point heat flux.

Radiant effects are generally not large, except for the 8410 W flame (Condition 8, Table 5) where radiation contributes about 30 percent of the stagnation point heat flux.

Figure 5 is an illustration of the radial variation of convective ceiling heat flux. The variation of total heat flux is qualitatively similar to the results shown in Fig. 5, but slightly higher due to the contribution of radiation. The theoretical prediction of Alpert [9, 10] for two different assumed values of ceiling friction factor, and the stagnation point correlation for two different values of  $Ra$ , are also shown on the figure. The experimental results from Refs. 23-25 are not shown, but these data generally fall between the limits of Alpert's theory. The data show large scatter, when plotted in this manner, with results at higher values of  $Ra$  tending to be lower at any value of  $r/H$ .

Figure 6 is a replot of the data, using the stagnation point heat flux parameter for the abscissa. This choice nicely collapses all the results in the ceiling jet region to a single line. In fact, the scatter is greatest in the stagnation region, where flow development and incomplete combustion effects exert the greatest influence. If the branch region  $0.04 < r/H < .3$  is approximated by the straight line segments illustrated in Fig. 6, the following correlation is obtained for the ceiling heat flux

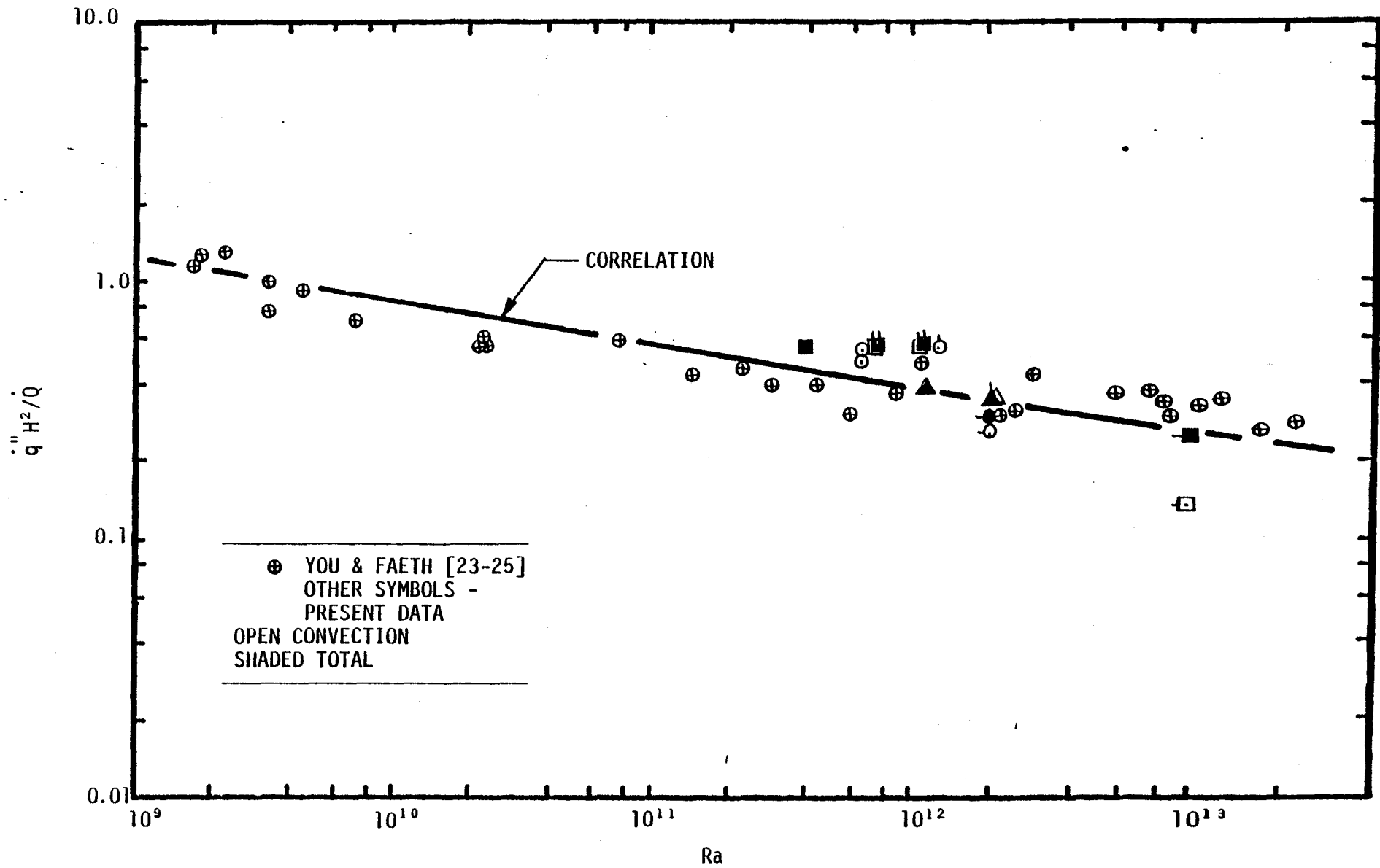


Figure 4. Convective and total heat flux at the ceiling stagnation point.

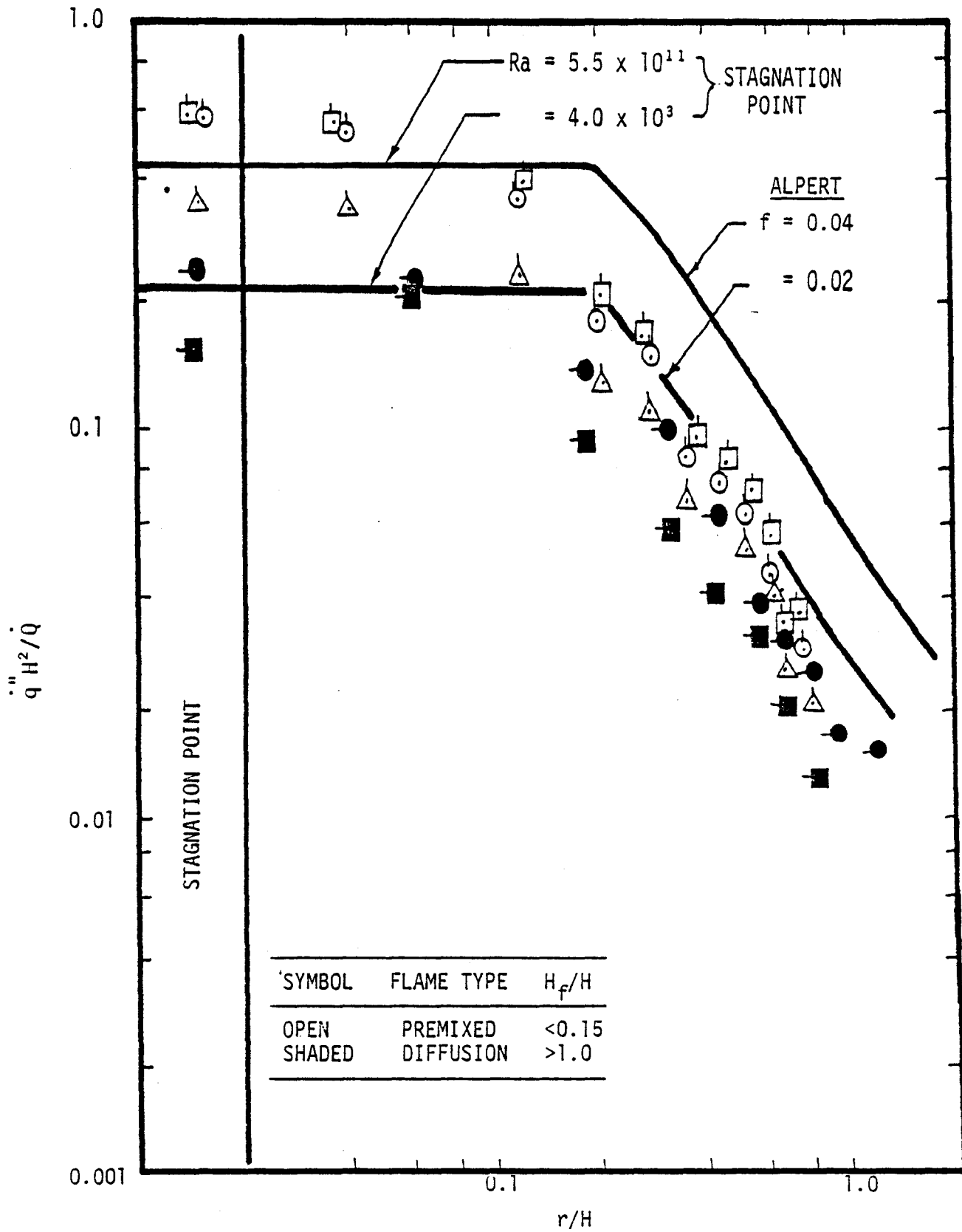


Figure 5. Radial variation of convective heat flux to the ceiling.

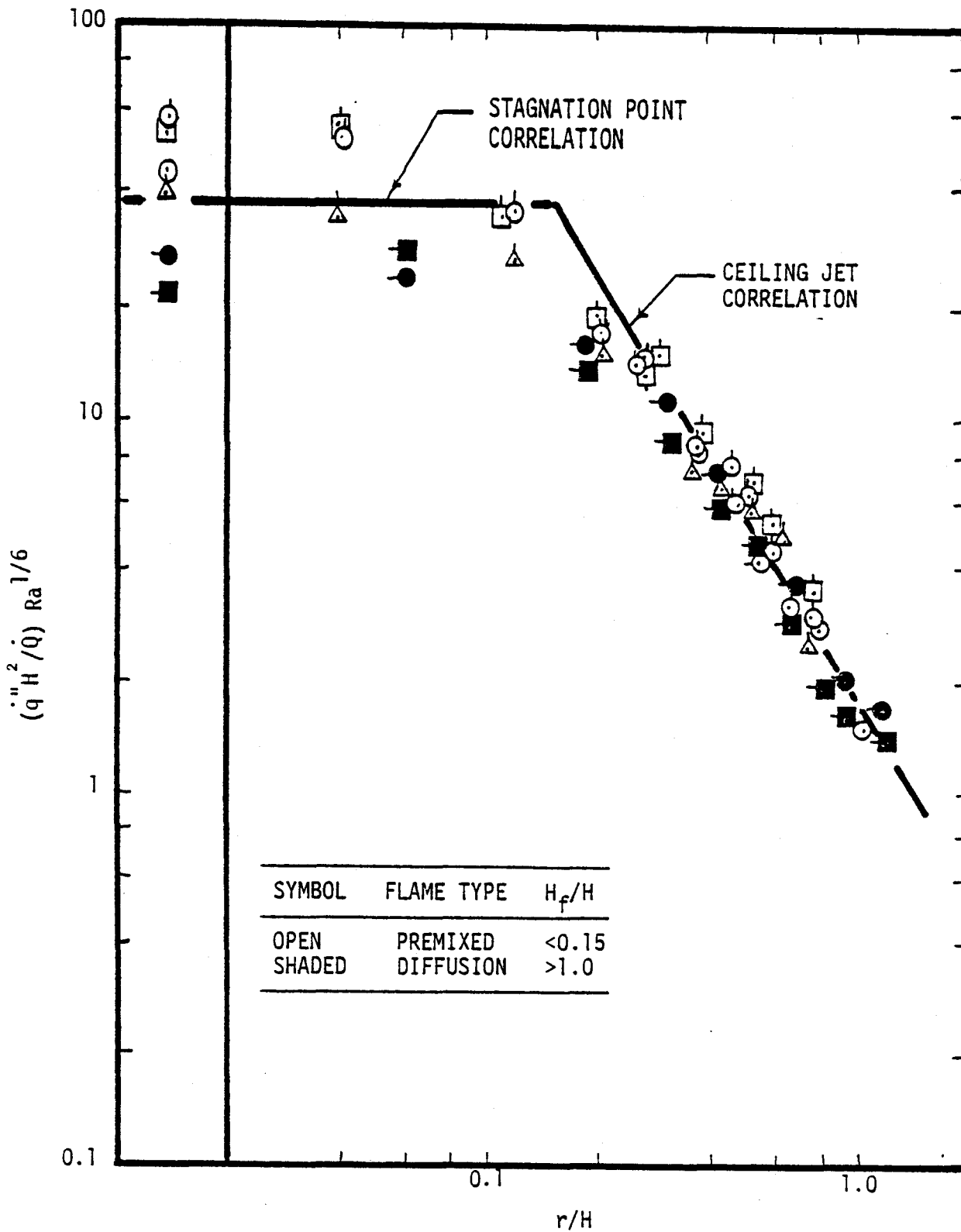


Figure 6. Correlation of convective heat flux to the ceiling.

$$\begin{aligned}
 (\dot{q}'' H^2 / \dot{Q}) Ra^{1/6} Pr^{3/5} &= 31.2, & r/H < 0.16 \\
 &= 1.46(r/H)^{-1.63}, & r/H < 0.16
 \end{aligned}
 \tag{1}$$

for the range  $10^9 < Ra < 10^{14}$ ,  $H_c/H < 1.5$ ,  $Pr \approx 0.7$ . Equation (1) only includes convection; any additional contribution due to radiation must be computed separately. The expression was developed for impingement on an unconfined ceiling. Earlier work suggests that heat fluxes for confined ceilings are somewhat higher than those for unconfined ceilings, although Eq. (1) represents a reasonable first estimate for the former case [23-25].

## 4.2 Flow Structure

Due to the substantial effort required for flow structure measurements, only the diffusion flames (conditions 7 and 8 in Table 5) were considered.

### 4.2.1 Flame Shape

Flame shape is a very subjective measurement for a turbulent flame. Nevertheless, the geometry of the luminous region is of some value in order to indicate the character of the flow. Two techniques were employed for these measurements, as described in Section 2.2: (1) visual observation, similar to the approach employed in Refs. 23-25, and (2) the determination of the boundaries of luminous zones on photographs.

The results for the two diffusion flames are illustrated in Figs. 7 and 8. Due to the fluctuating nature of the flow, the data are indicated by bounds. The photographs were obtained with Polaroid Type 52 film employing a Graphlex 4 x 5 still camera set at  $f = 4.7$  with an exposure time of 0.04s. Any other setting would result in a shift of the boundaries. The exposure time was chosen to roughly correspond to the time constant of the human eye. For these conditions, the flame shape found from the photographs was generally narrower than the shape obtained from direct visual observation.

Gas velocities leaving the burner are relatively low, in order to simulate a natural fire. Therefore, the flame radius contracts for a time near the burner exit, as the flow accelerates due to buoyancy forces. A minimum flame radius is reached about one burner radius above the burner exit. Above this region, the flame radius grows again, in response of the radial growth of the flow as a result of entrainment.

The maximum flame radius, in the plume portion, occasionally reaches  $r/z = 0.4$ , for both flames. Condition 7 represents a case where the flame tip just impinges on the ceiling. For condition 8, the flame generally impinges on the ceiling and occasional luminous zones are observed out to  $r/H = 0.73$ . The lower extremity of the impinging flame occasionally reaches  $y/H = 0.12$ . Later results will show that these zones of occasional luminosity extend to the boundaries of the mean temperature disturbance.

### 4.2.2 Mean Temperatures

Temperature distributions in the plume and the ceiling jet regions of the flow will be considered separately.

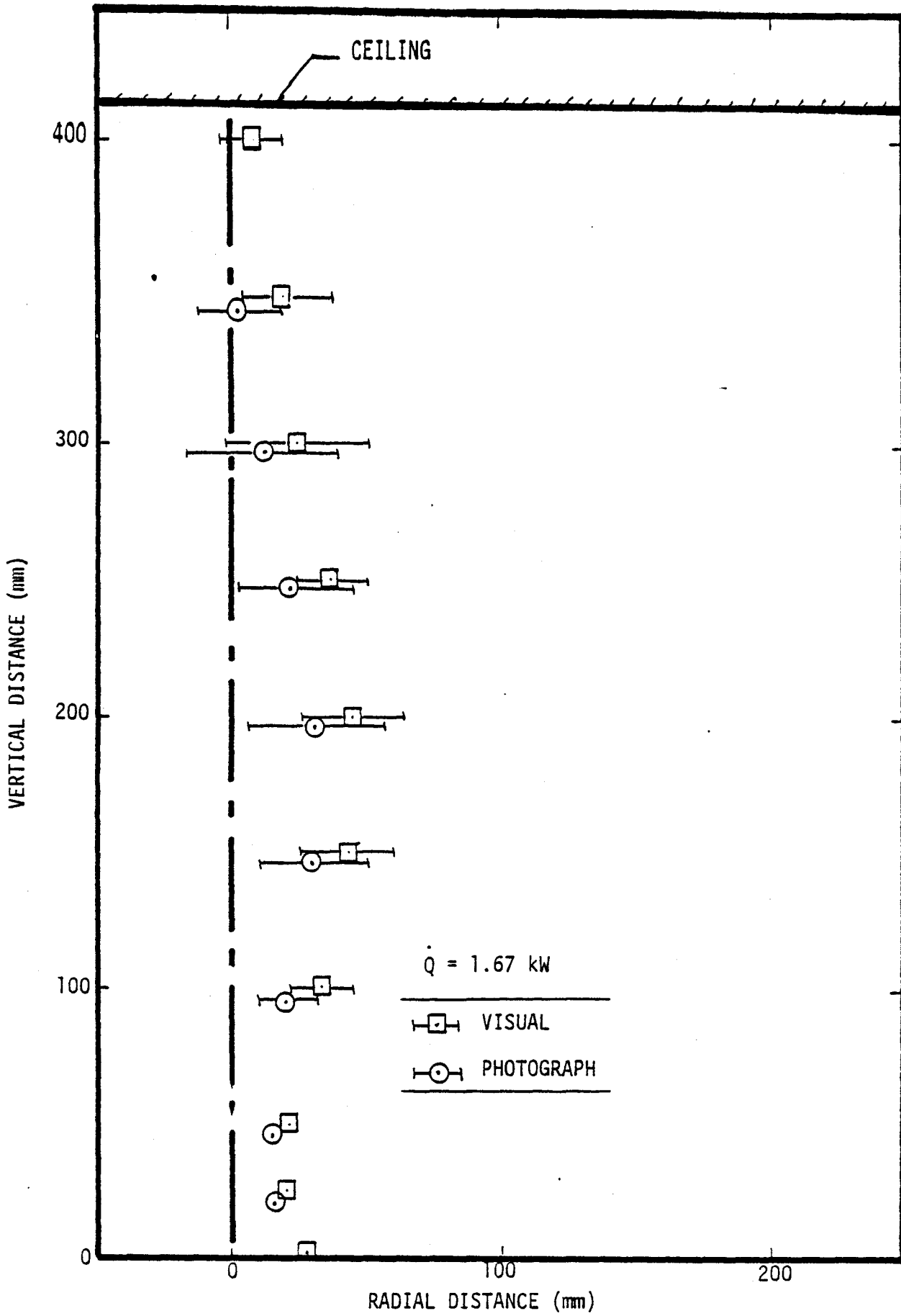


Figure 7. Flame shape, 1.67 kW fire (condition).

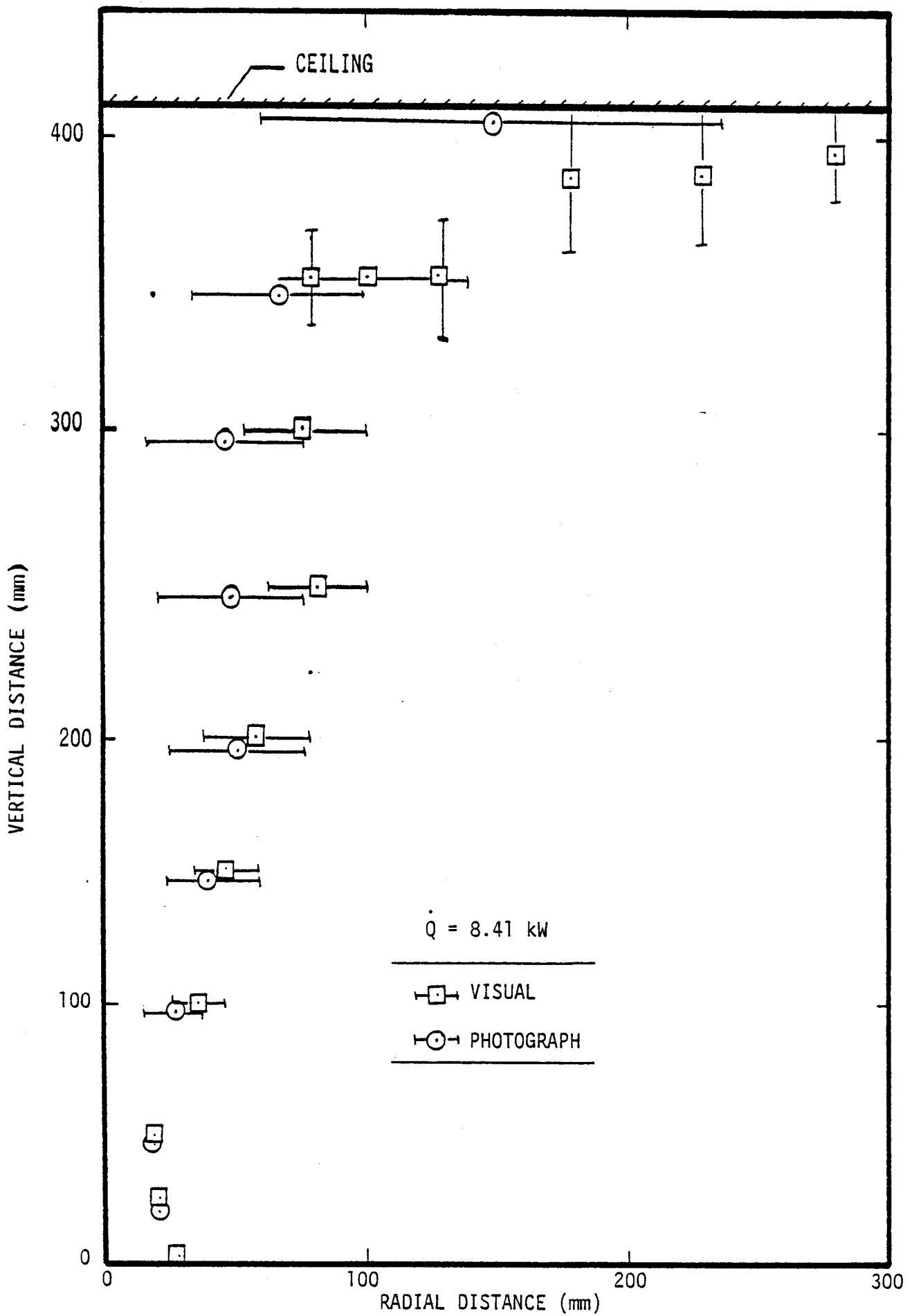


Figure 8. Flame shape, 8.41 kW fire (condition 8).

Plume. Mean temperatures along the axis of the fire plume are illustrated by Fig. 9. Results from our earlier study [23-25], McCaffrey [12], and Cox and Chitty [13] are also illustrated on the figure. The latter two studies employed the same apparatus. Theoretical predictions obtained from Rouse, Yih and Humphreys [19] and Yokoi [21] are also illustrated. These results are limited to the noncombusting portions of the flow. The coordinate axes of Fig. 9 are dimensional, however, the form of the variables generally rests on scaling rules appropriate for noncombusting plumes [12,13].

Mean temperatures are variable near the burner exit, from case to case. (Data from Refs. 12 and 13 are not included in this region to avoid cluttering the figure, the original references should be consulted for the details). This region is not a boundary layer flow, c.f. Figs. 7 and 8, and similarity of profiles is not expected in coordinates based on far field scaling. Furthermore, laminar flow effects are also observed here, reducing the likelihood of scaling with turbulent flow parameters.

One factor that is not observed in the present data involves the relatively constant temperature region for  $.03 < z/Q^{2/5} < 0.08$ , which was reported in Refs. 12 and 13. The present data shows a monotonic increase in temperature, near the burner, with the temperature reaching a maximum at  $z/Q^{2/5} = 0.1$ . Increasing the strength of the fire causes the slope of this curve to increase. These differences are felt to be due to the nature of the burner. A porous refractory burner was used in Refs. 12 and 13, while the present tests employed an open tube, covered with a fine mesh screen. The former arrangement would provide more effective heating of the fuel gases, since the burner face is heated by radiation from the flame, and the porous structure provides an effective agent for heat transfer between the burner face and the fuel gases.

The present maximum mean temperature levels are higher than those of Refs. 12 and 13, and remain higher in the region  $z/Q^{2/5} > 0.1$ . Natural gas was employed as the fuel in all cases and it seems unlikely that variations in fuel properties are responsible for these differences. The effect may be the result of instrumentation. In particular, Cox and Chitty [13], employed a relatively large thermocouple junction, in comparison to the present arrangement. Larger radiation errors from the larger junction would result in lower indicated gas temperatures.

Axial temperatures in the plume, measured during the initial phases of this study [23-25], agree quite well with the correlation due to Rouse, et al. [19]. These measurements were in the noncombusting portion of the flow, at some distance from the flame, where maximum temperature levels are relatively low. The correlation of Ref. 19 was developed for the weakly buoyant region of the flow, and this type of agreement is to be expected. The recent measurements are nearer the tip of the flame, in the strongly buoyant region, where the approximations employed by Rouse, et al [19], begin to break down. In view of this, the agreement between the data and the correlation is surprisingly good, although the correlation tends to underestimate the measurements.

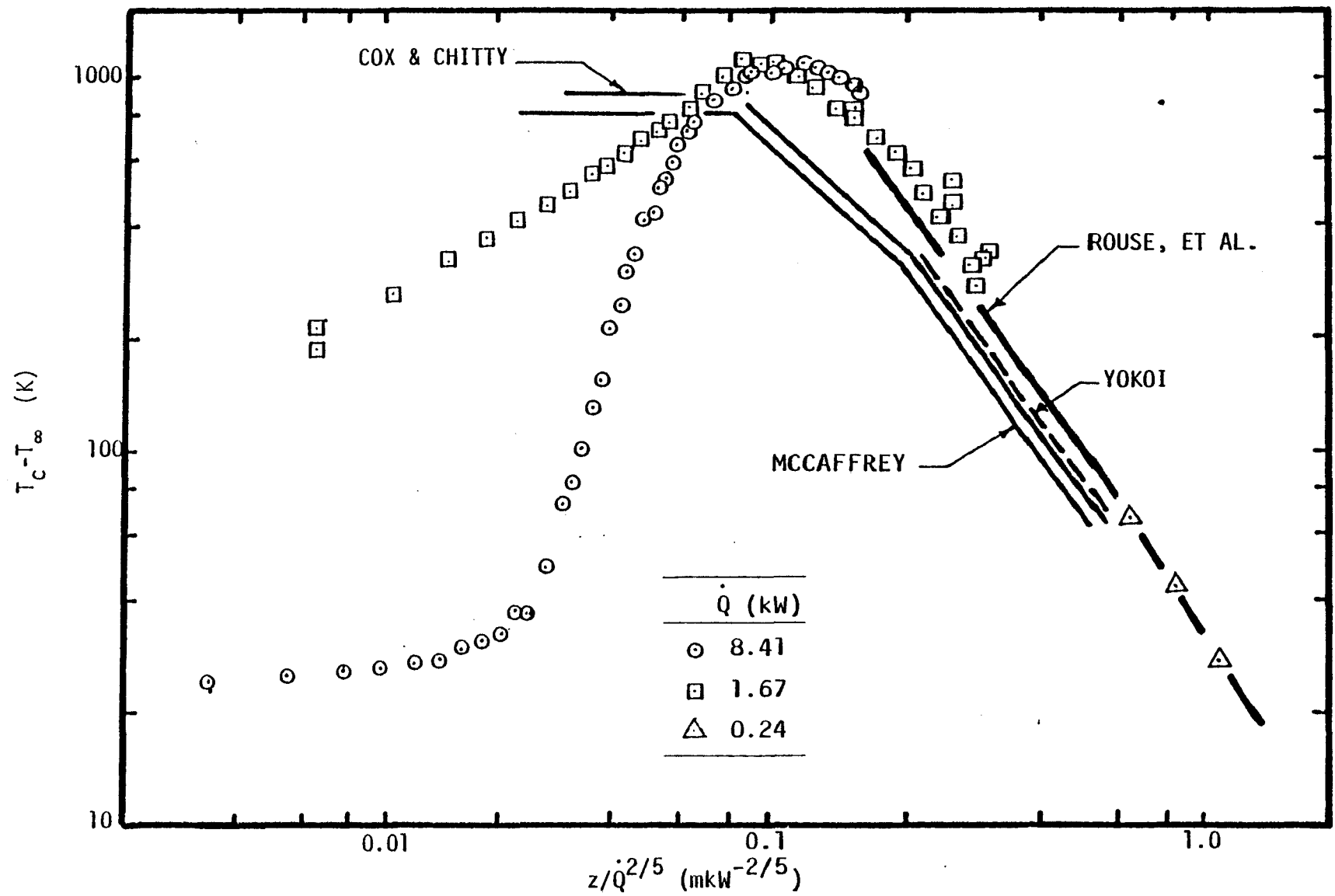


Figure 9. Mean temperature variation along the flame axis.

The plume correlations can be placed in the form used in Fig. 9 as follows:

$$T_c - T_\infty = C_T (g\beta\rho^2 C_p^2)^{-1/3} (z/\dot{Q}^{2/5})^{-5/3} \quad (2)$$

$$w_c/\dot{Q}^{1/5} = C_W (g\beta/\rho C_p)^{1/3} (z/\dot{Q}^{2/5})^{-1/3} \quad (3)$$

where the values of  $C_T$  and  $C_W$  from various investigators are summarized in Table 6. Since the equations were developed for the weakly buoyant region, ambient properties are used. Considering Eq. (2) for axial temperatures, there is a tendency for the temperature difference to increase as the temperature at which properties are evaluated is increased. The ambient temperature has been used when the correlation was plotted in Fig. 9, thus the correlations are as low as possible on the figure. Viewed in this light, it is not surprising that the values near the tip of the flame, where a higher temperature for property evaluation would be more appropriate, lie above the correlation. The data of Refs. 12 and 13 fit the correlation of Yokoi [21], by virtue of the fact that his coefficient,  $C_T$ , is lower, c.s. Table 6. The fact that this data doesn't tend to rise above the line, at higher centerline temperatures, may be the result of the temperature measurement errors discussed earlier.

Figures 10 and 11 are illustrations of mean temperature profiles at various positions in the 1.67 and 8.41 kW fires. The results are qualitatively similar to findings in combustng jets [32]. There is a core of cooler gas near the exit of the burner. Maximum mean temperature levels are below adiabatic flame temperature levels due to turbulent mixing. Comparison of Figs. 7 and 8, and Figs. 10 and 11, indicates that occasional flame luminosity extends the full width of the thermal disturbance, in the combustng region of the flow. In terms of  $r/x$ , the flow width in the combustng region is somewhat larger than is the case for noncombustng plumes [19,20]. The profile at 365 mm for the 8.41 kW fire (Fig. 11), extends to the edge of the ceiling jet. In this case, the temperature defect does not approach zero near the edge of the flow.

Ceiling Jet. Figures 12 and 13 illustrate mean temperature profiles in the ceiling jet for conditions 7 and 8. The general features of these results are similar to earlier findings for impinging plumes [9-11,23]. The thickness of the layer is increased, however, for flame impingement, c.f. Fig. 13. This characteristic is similar to the flaming portions of the plume, which are generally thicker, in terms of  $r/x$ , than noncombustng flows. The temperature profile near the wall becomes steeper with greater radial distance along the ceiling. This behavior was also observed in wall plumes [33,34]. This suggests that local similarity is only approximate in the ceiling layer. A detailed comparison of these measurements with existing theory is currently in progress and will be reported later.

#### 4.2.3 Mean and Fluctuating Velocities

Test results for mean and fluctuating velocities in the plume and ceiling jet regions will be discussed separately.

TABLE 6  
Plume Profile Constants

Source	$C_w$	$C_T$
Rouse, et al [19]	4.7	11.0
George, et al. [20]	3.4	9.0
Yokoi [21]	3.8	9.1

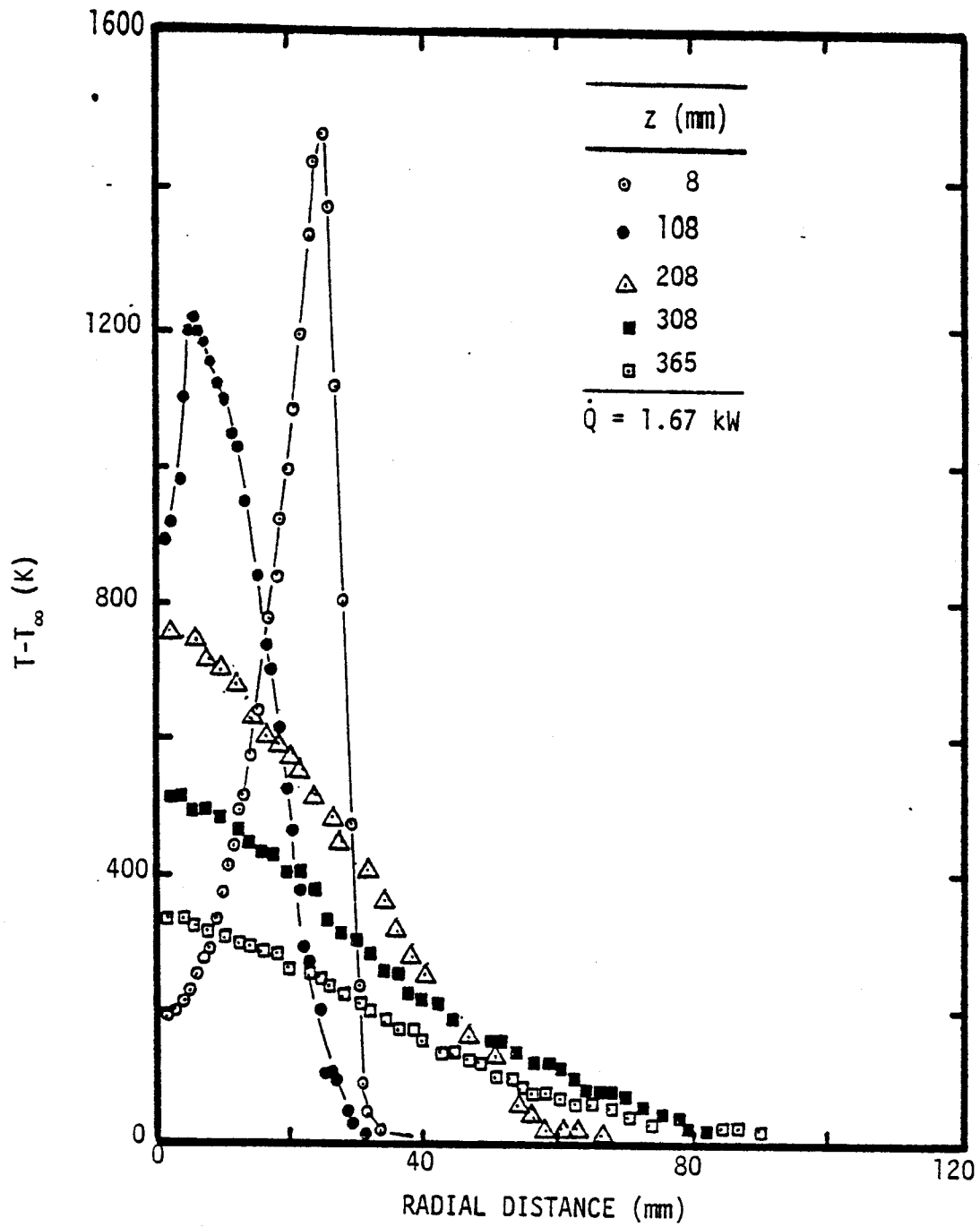


Figure 10. Radial mean temperature profiles, 1.67 kW fire (condition 7).

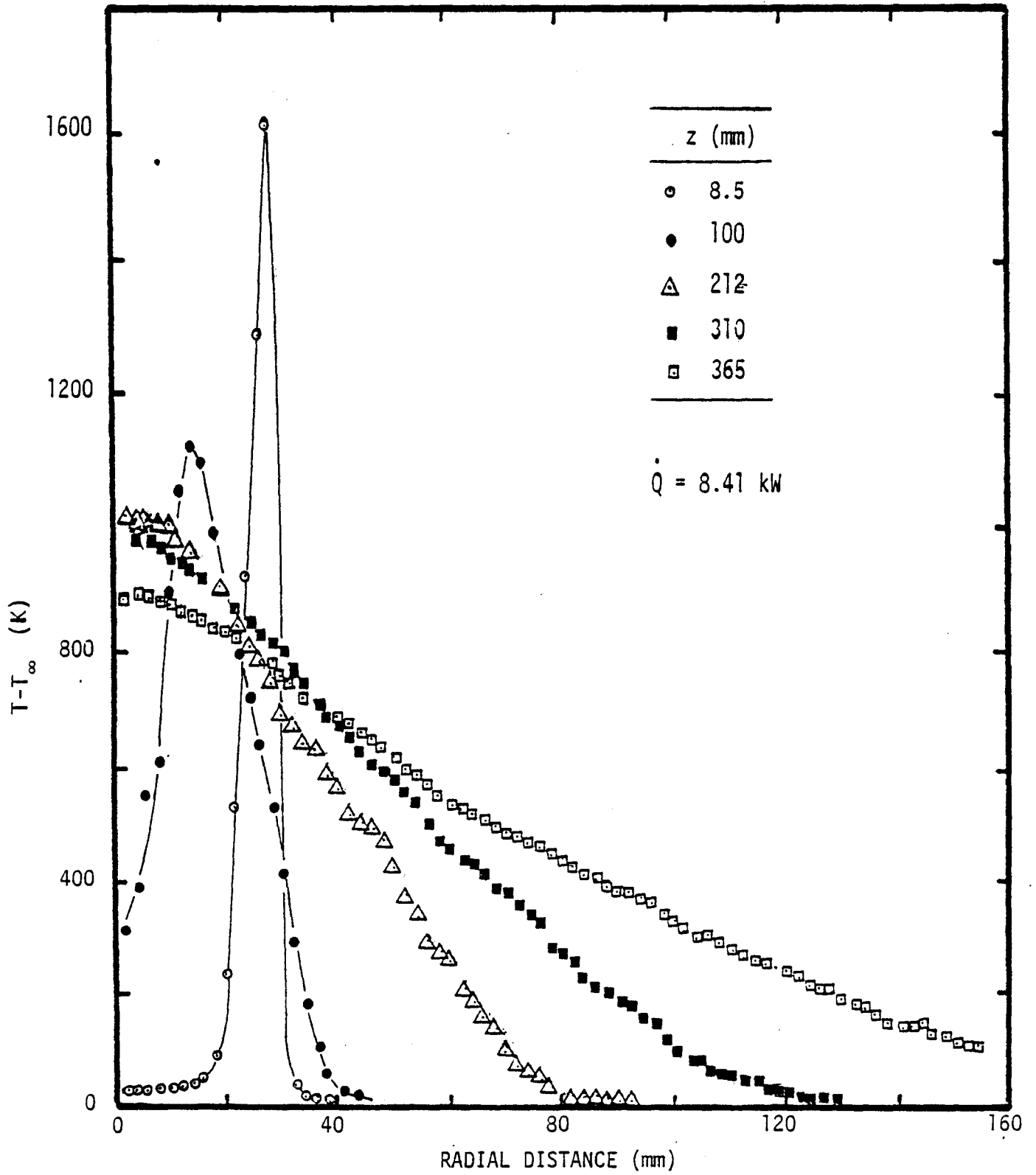


Figure 11. Radial mean temperature profiles, 8.41 kW fire (condition 8).

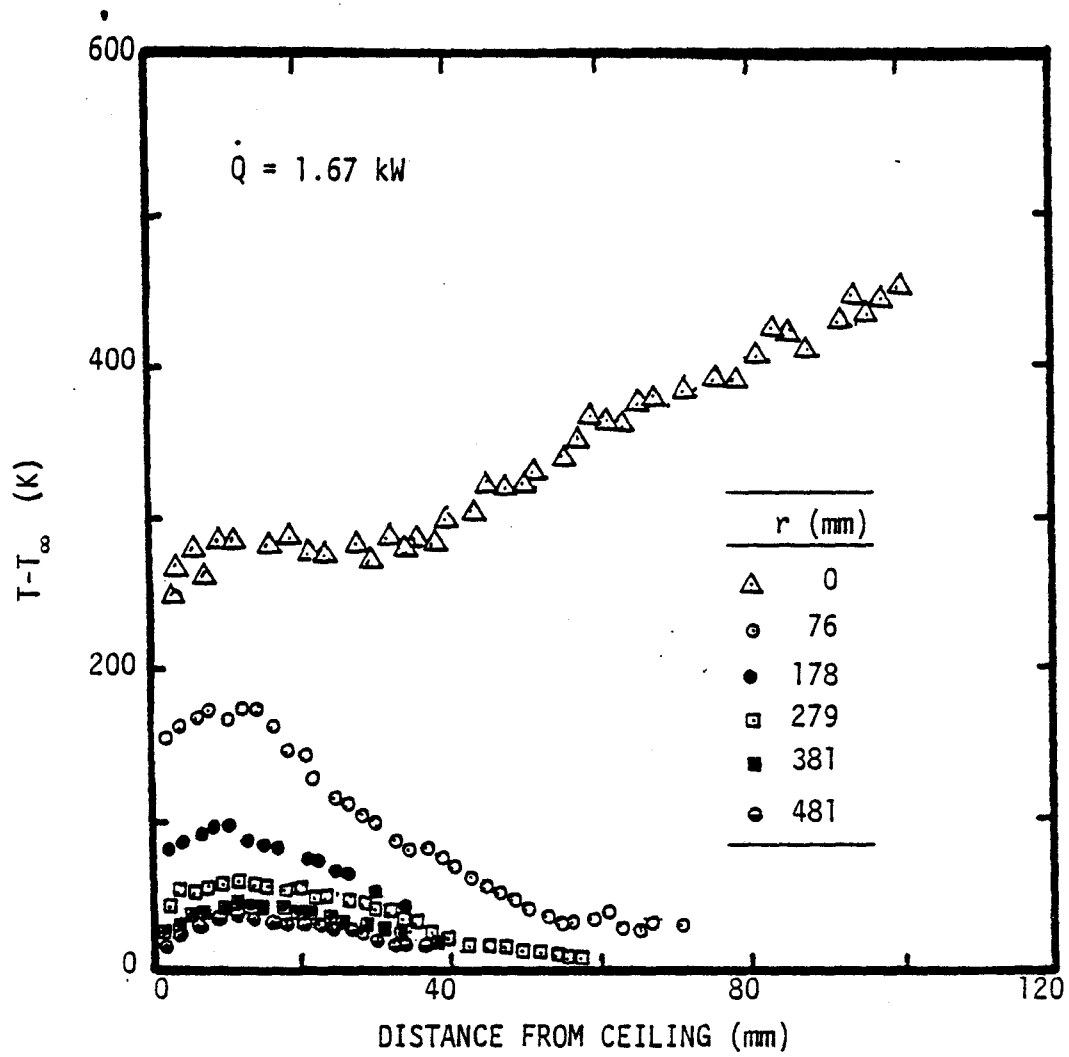


Figure 12. Mean temperature profiles in the ceiling jet, 1.67 kW fire (condition).

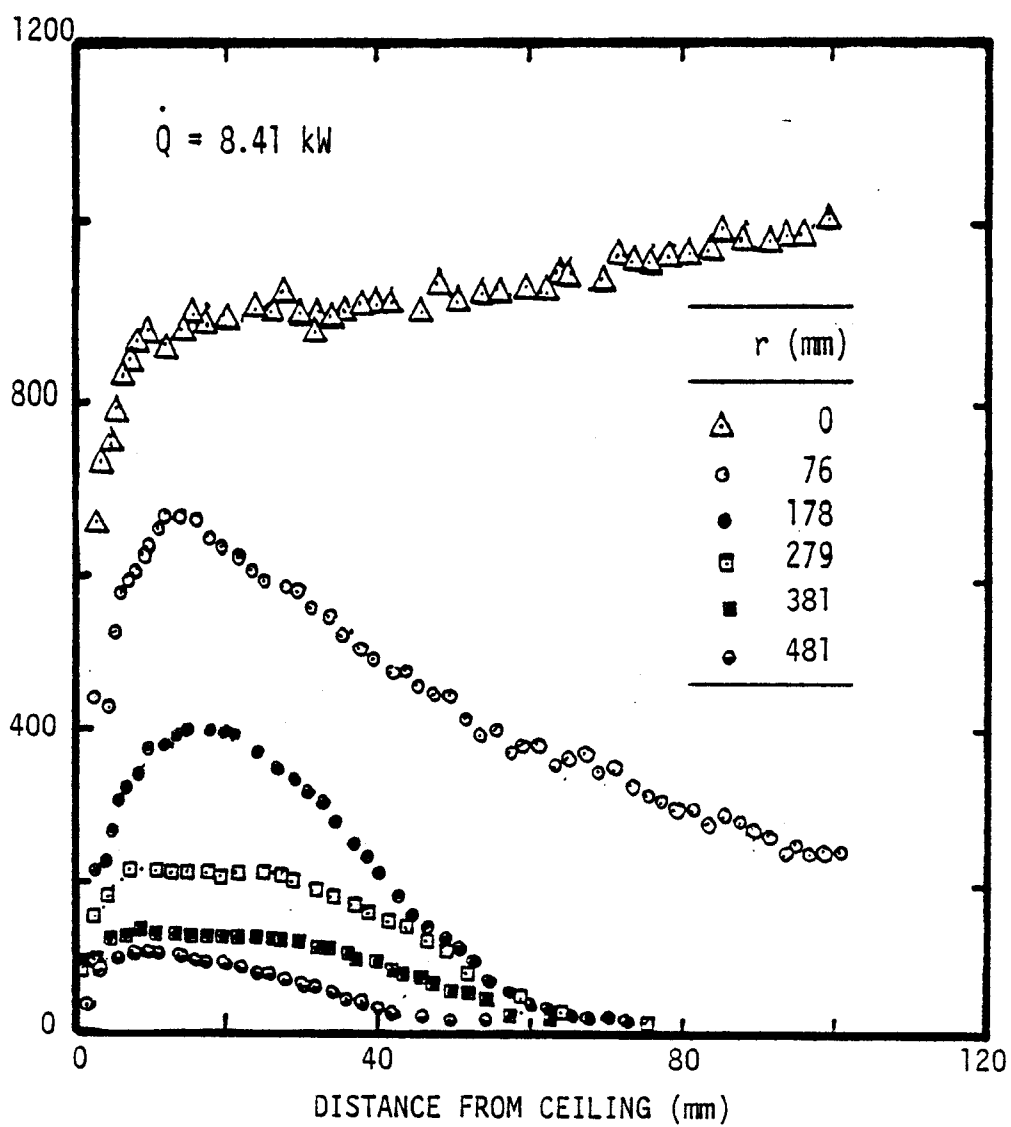


Figure 13. Mean temperature profiles for the ceiling jet, 8.41 kW fire (condition 8).

Plume. In order to gain familiarity with the LDA measurements, an initial series of experiments were conducted using a nonflaming buoyant source. This involved a flow of helium from a 10 mm I.D. tube. The helium flow rate was adjusted to provide a Froude number at the exit of the tube which corresponds to the asymptotic Froude number of a fully developed plume. In this circumstance, overall acceleration and deceleration of the flow is unnecessary, which reduces the length required for flow development [20].

Figure 14 is an illustration of the mean velocity profiles obtained in the helium plume. Various axial positions above the source are considered. The coordinate system for the plot employs the similarity variables of fully developed plumes [19]. In addition to the present data, correlations obtained from earlier studies [19,20] are also illustrated. The present measurements agree best with the results of George, et al. [20], near the centerline of the flow. However, near the edge of the plume, the present measurements approach the results of Rouse, et al. [19]. The fact that current measurements of mean velocity are lower than those of George, et al. [20] near the edge of the flow is to be expected. A hot wire anemometer was employed for the measurements of Ref. 20, which cannot detect flow reversals, yielding a higher mean velocity than the true value in the edge region. The three sets of measurements illustrated in Fig. 14 suggest similarity of the flow.

Turbulent fluctuations  $w'$  and  $v'$ , as well as the Reynolds stress, were also measured in the plume. As a sample of this data, longitudinal velocity fluctuations are illustrated in Fig. 15. Hot wire measurements of George, et al. [20] are also illustrated on the figure. The velocity fluctuations exhibit similarity when plotted in the coordinate system of Fig. 15. However, present measurements are somewhat higher than those of Ref. 20, near the centerline of the flow, and a reduction in the longitudinal intensity near the centerline is less pronounced.

Figure 16 is an illustration of mean velocity measurements along the axis of the flame. The present data includes conditions 7 and 8 (Table 5) as well as results in the helium plumes. Results from other investigations include Cox and Chitty [13], McCaffrey [12], Thomas [35], Yokoi [21], Rouse, et al. [19] and George, et al. [20]. The present data falls along the line obtained by Thomas [35], in the region near the burner surface. A greater degree of similarity between the two test flames is observed for velocities than was the case for mean temperatures. The current measurements are lower than those of Refs. 12 and 13 in the near burner region, which again may be an artifact of the burner design and operating conditions. The present results agree best with the correlation of George, et al. [20], in the region far from the source.

Considering the results of Figs. 9 and 16 together, for three regime structure for a natural fire, suggested by McCaffrey [12], is observed. This corresponds to a region of increasing temperatures and velocities near the source; a region where temperatures and velocities vary relatively slowly, near the flame tip; and a region of decaying temperature and velocity, in the noncombusting plume. The details of each of these zones vary from investigation to investigation, particularly near the fire source. This state of affairs is an impediment to progress in understanding fire impingement, since the plume provides the initial condition for the ceiling flow.

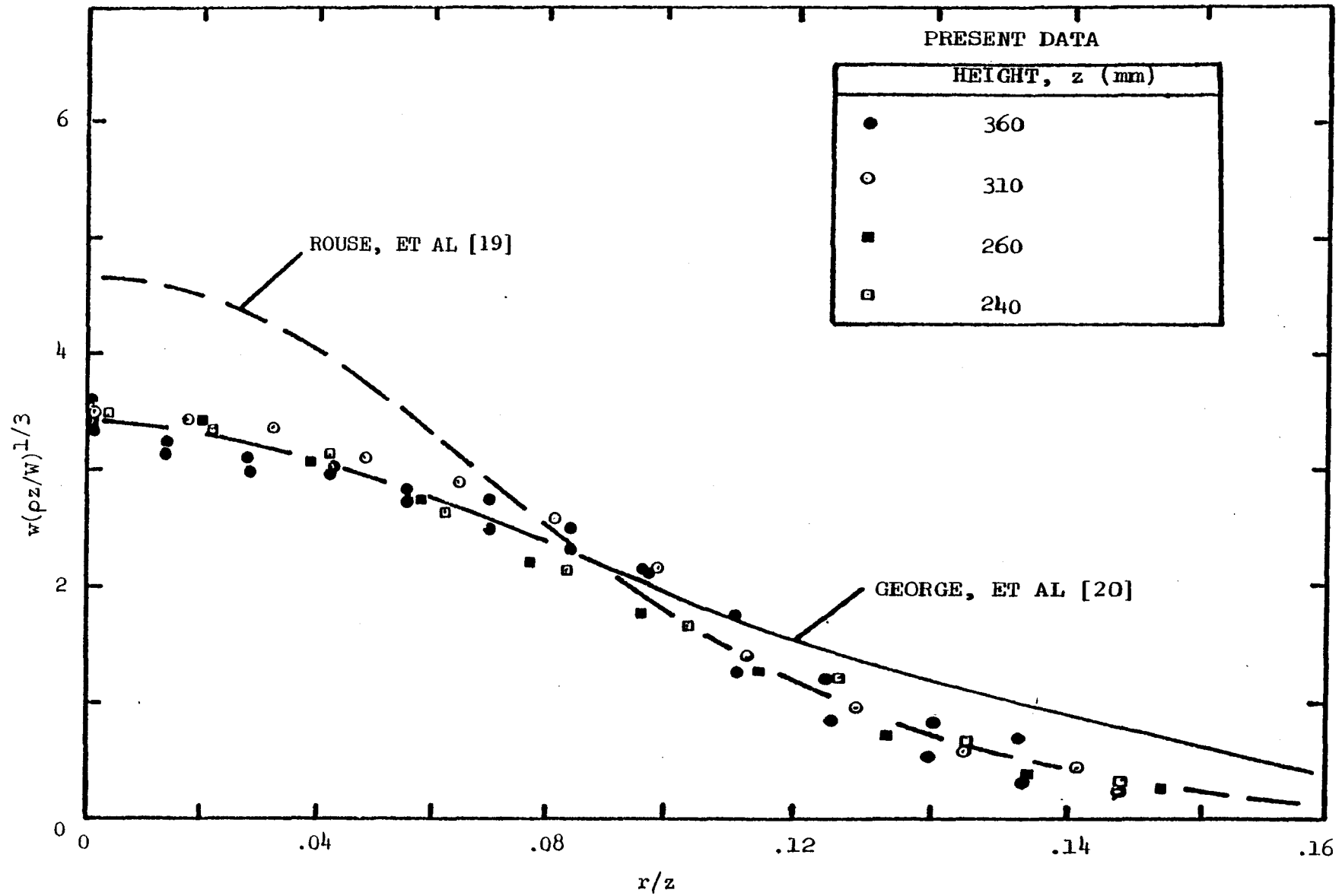


Fig. 14 Mean velocity measurements using the LDA in a buoyant plume.

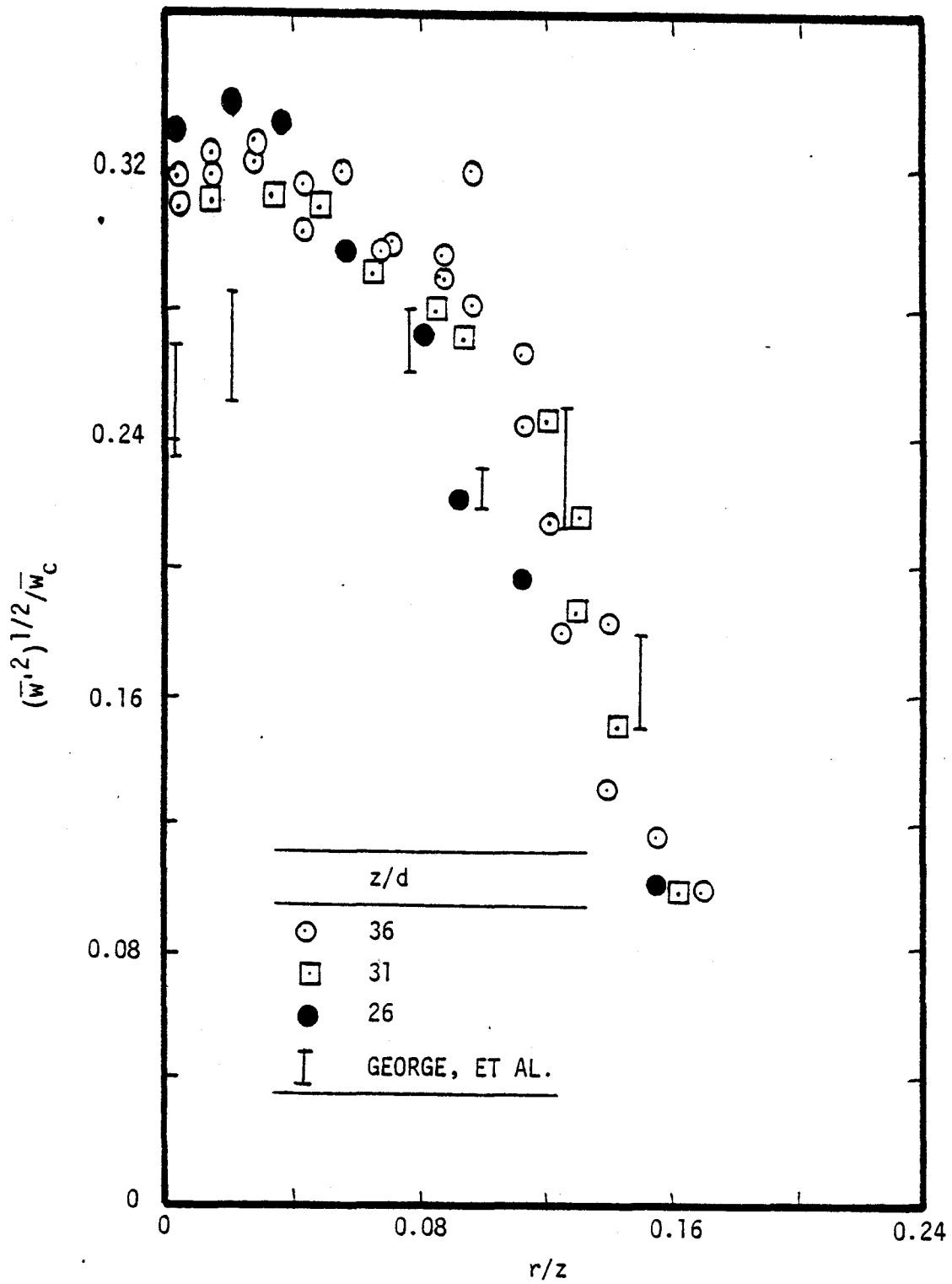


Figure 15. Longitudinal velocity fluctuations in a buoyant plume.

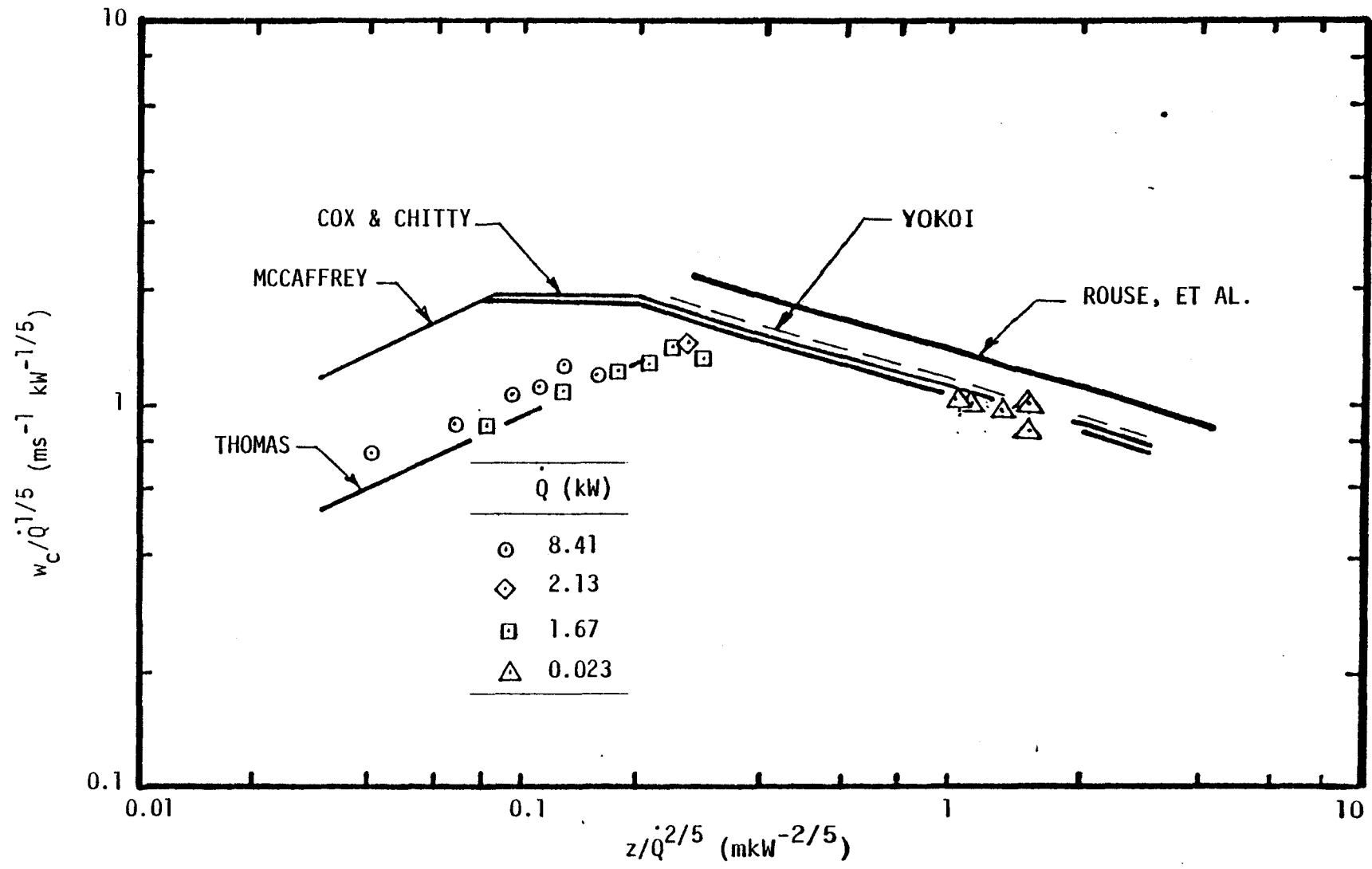


Figure 16. Mean velocity variation along the flame axis.

Measurements of mean velocity, velocity fluctuation and Reynolds stress profiles were also completed for the two diffusion flames. Complete reporting of these results will be deferred until all the structure measurements are complete. Some notable features, however, are that velocity profiles extend to  $r/z = 0.35$  in the combusting portion of the flow, as opposed to  $r/z = 0.20$  in the noncombusting plume (Fig. 14). Similarity is not observed in the combusting plume region, low Reynolds numbers, flow development and combustion all affect the turbulent structure of the flow.

Ceiling Jet. Measurements in the ceiling jet were completed for the impinging helium plume. Mean velocities, velocity fluctuations and Reynolds stress profiles were obtained for  $r/H$  in the range 0.1-0.40, using the LDA. A complete report of these results will be deferred until the measurements in the combusting flows are concluded. Mean velocities are strongly decelerating with maximum velocities decreasing by almost an order of magnitude in the range  $r/H = 0.1-0.4$ . Mean velocities were only 50-70% as large as the values reported by Alpert [9,10], for comparable conditions. This is not surprising, since turbulent intensities are on the order of 100% over much of this region. Alpert's results were obtained with a hot wire, which tends to overestimate the mean velocity in a high turbulence intensity flow, as noted earlier.

The initial experience with the LDA in the ceiling jet region indicated several problem areas. The long beam path lengths, with our arrangement, through a turbulent variable density medium, limits the accuracy of the measurement of turbulent quantities. The current arrangement also requires that the ceiling be moved in order to complete profile measurements. Due to the relatively large size of the apparatus, this is difficult to do accurately. In view of these problems, subsequent velocity measurements in the ceiling jet will employ the impact probe, similar to earlier work on combusting wall plumes [29]. Impact probes are subject to errors in high turbulence intensity flows, however, this effect can be calibrated by comparison with the LDA measurements in the plume.

#### 4.2.4 Radiation Measurements

Radiation measurements have been completed for the two diffusion flames. Reporting of these results will be deferred pending completion of composition measurements. The availability of complete structure measurements will provide a rational basis for comparison between predicted and measured radiant heat fluxes.

REFERENCES

1. H. W. Emmons, H. E. Mitler and L. N. Trefethen, "Computer Fire Code III," Home Fire Technical Report No. 25, Harvard University, Cambridge, MA (1978).
2. E. E. Zykoski and T. Kubota, "A Computer Model for Fluid Dynamic Aspects of a Transient Fire in a Two Room Structure," Report under USDC-NBS, Center for Fire Research Grant No. 5-9004, California Institute of Technology, Pasadena, CA (1978).
3. E. E. Smith and M. J. Clark, "Model of the Developing Fire in a Compartment," ASHRAE Trans. 81, Part I, 568, (1975).
4. A. C. Ku, M. L. Doria, and J. R. Lloyd, "Numerical Modeling of Unsteady Buoyant Flows Generated by Fire in a Corridor," Sixteenth Symposium (International) on Combustion, The Combustion Institute, Pittsburgh, PA, 1373 (1977).
5. T. Tanaka, "A Mathematical Model of a Compartment Fire," Second Joint Meeting, U.S.-Japan Panel on Fire Research and Safety, UJNR, Tokyo (1976).
6. J. Prah1 and H. W. Emmons, "Fire Induced Flow through an Opening," Combustion and Flame, Vol. 25, pp. 369-385 (1975).
7. P. H. Thomas, J.F.R.O. Note No. 141, Fire Research Station, Boreham Wood, Herts, England (1955).
8. R. W. Pickard, D. Hird, and P. Nash, J.F.R.O. Note No. 247, Fire Research Station, Boreham Wood, Herts, England (1957).
9. R. L. Alpert, "Fire Induced Turbulent Ceiling-Jet," Technical Report No. 19722-2, Faculty Mutual Research Corporation, Norwood, MA (1971).
10. R. L. Alpert, "Turbulent Ceiling-Jet Induced by Large-Scale Fire," Technical Report No. 22357-2, Factory Mutual Research Corporation, Norwood, MA (1974).
11. E. E. Zukoski, T. Kubota and C. C. Veldman, "Experimental Study of Environment and Heat Transfer in a Room Fire," Technical Report No. 1, Grant No. 5-9004, California Institute of Technology, Pasadena, CA (1975).
12. B. J. McCaffrey, "Purely Buoyant Diffusion Flames: Some Experimental Results," 1978 Fall Technical Meeting, Eastern Section of The Combustion Institute, Miami Beach, FL, pp. 8-1 to 8-4, Nov.-Dec., 1978.
13. G. Cox and R. Chitty, "A Study of the Deterministic Properties of Unbounded Fire Plumes," to be published.

15. A. A. Putnam and C. F. Speich, "A Model Study of the Interaction of Multiple Turbulent Diffusion Flames," Ninth Symposium (International) on Combustion, Academic Press, New York, 867 (1963).
16. F. J. Kosdon, F. A. Williams and C. Buman, "Combustion of Vertical Cellulosic Cylinders in Air," Twelfth Symposium (International) on Combustion, The Combustion Institute, Pittsburgh, 253 (1969).
17. F. R. Steward, "Prediction of the Height of Turbulent Diffusion Buoyant Flames," Comb. Sci. and Tech. 2,203 (1970).
18. D. C. Wilcox, "Model for Fires with Low Initial Momentum and Nongray Thermal Radiation," AIAA J. 13, 381 (1975).
19. H. Rouse, C. S. Yih and H. W. Humphreys, "Gravitational Convection from a Boundary Source," Tellus 4, 201 (1952).
20. W. K. George, R. L. Alpert, and F. Tamanini, "Turbulence Measurements in an Axisymmetric Buoyant Plume," Int. J. Heat Mass Transfer 11, 1145 (1977).
21. S. Yokoi, "Student on the Prevention of Fire Spread Caused by Hot Upward Current," Report No. 34, Building Research Institute, Japanese Government, November 1960.
22. P. H. Thomas, R. Baldwin and A. T. M. Heselden, "Buoyant Diffusion Flames: Some Measurements of Air Entrainment, Heat Transfer, and Flame Merging," Tenth Symposium (International) on Combustion, The Combustion Institute, Pittsburgh, 983 (1965).
23. H-Z. You and G. M. Faeth, "An Investigation of Fire Impingement on a Horizontal Ceiling," Report under USDC-NBS Center for Fire Research Grant No. 7-9020, The Pennsylvania State University, University Park, PA (1978).
24. H-Z. You and G. M. Faeth, "Fire Impingement on a Ceiling," 1978 Technical Meeting, Eastern Section of the Combustion Institute, Miami Beach, Florida, November 1978.
25. H-Z. You and G. M. Faeth, "Ceiling Heat Transfer during Fire Plume and Fire Impingement," J. of Fire and Materials, in press.
26. J. A. Liburdy and G. M. Faeth, "Fire Induced Plumes Along a Vertical Wall: Part I. The Turbulent Weakly Buoyant Region," Report under USDC-NBS, Center for Fire Research Grant 5-9020, The Pennsylvania State University, University Park, Pennsylvania (1977).
27. A. J. Shearer, H. Tamura and G. M. Faeth, "Evaluation of a Locally Homogeneous Flow Model of Spray Evaporation," J. of Energy, in press.

28. F. Durst and J. H. Whitelaw, "Measurements of Mean Velocity, Fluctuating Velocity and Shear Stress in Air using a Single Channel Optical Anemometer," DISA Information No. 12, 11 (1971).
29. T. Ahmad and G. M. Faeth, "Turbulent Wall Fires," Seventeenth Symposium (International) on Combustion, The Combustion Institute, Pittsburgh, 1149 (1979).
30. L. Orloff, J. de Ris and G. H. Markstein, "Upward Turbulent Fire Spread and Burning of Fuel Surface," Fifteenth Symposium (International) on Combustion, The Combustion Institute, Pittsburgh, 183 (1974).
31. C. DuP. Donaldson, R. S. Snedeker and D. P. Margolis, "A Study of Free Jet Impingement, Part 2. Free Jet Turbulent Structure and Impingement Heat Transfer," J. Fluid Mech. 45, 477 (1971).
32. C-P. Mao, G. A. Szekely, Jr., and G. M. Faeth, "Evaluation of a Locally Homogeneous Flow Model of Spray Combustion," NASA CR 3202 (1979).

U.S. DEPT. OF COMM. BIBLIOGRAPHIC DATA SHEET	1. PUBLICATION OR REPORT NO. NBS-GCR-80-251	2. Gov't Accession No.	3. Recipient's Accession No.	
4. TITLE AND SUBTITLE AN INVESTIGATION OF FIRE IMPINGEMENT ON A HORIZONTAL CEILING		5. Publication Date JULY 1980	6. Performing Organization Code	
7. AUTHOR(S) H-Z. You and G.M. Faeth	8. Performing Organ. Report No.			
9. PERFORMING ORGANIZATION NAME AND ADDRESS National Bureau of Standards Department of Commerce Washington, DC 20234		10. Project/Task/Work Unit No.	11. Contract/Grant No.	
12. Sponsoring Organization Name and Complete Address (Street, City, State, ZIP) The Pennsylvania State University Department of Mechanical Engineering University Park, PA		13. Type of Report & Period Covered	14. Sponsoring Agency Code	
15. SUPPLEMENTARY NOTES				
<p>16. ABSTRACT (A 200-word or less factual summary of most significant information. If document includes a significant bibliography or literature survey, mention it here.)</p> <p>This report covers the second year of a three-year study. The first year of the investigation was devoted to convective ceiling heat flux measurements. The present effort concentrated on radiative heat flux measurements and a portion of the flow structure measurements.</p> <p>A new experimental apparatus was constructed which allows the long term testing needed for structure measurements. This arrangement has a water-cooled ceiling, 1 m in diameter. The fire source is simulated by a 55 mm ID burner fueled with natural gas operating at heat release rates up to 8.5 kW. Convective and radiative heat fluxes are measured with heat flux gages, mean gas temperatures were obtained with fine wire thermocouples, mean velocities and velocity fluctuations are measured with a laser Doppler anemometer, an impact probe is also used for mean velocities, and mean concentrations are measured by isokinetic gas sampling with gas chromatograph.</p> <p>Measurements completed to date include: flame shape, convective and radiative heat fluxes to the ceiling, radiative heat fluxes to the ambiance, mean temperatures, and mean velocities and velocity fluctuations in the plume portion of the flow.</p>				
<p>17. KEY WORDS (six to twelve entries; alphabetical order; capitalize only the first letter of the first key word unless a proper name; separated by semicolons)</p> <p>Flame impingement, heat transfer, convection, radiation, temperature, velocity, field, ceilings.</p>				
<p>18. AVAILABILITY <input checked="" type="checkbox"/> Unlimited</p> <p><input type="checkbox"/> For Official Distribution. Do Not Release to NTIS</p> <p><input type="checkbox"/> Order From Sup. of Doc., U.S. Government Printing Office Washington, D.C. 20402, SD Cat. No. C13</p> <p><input checked="" type="checkbox"/> Order From National Technical Information Service (NTIS) Springfield, Virginia 22151</p>	<p>19. SECURITY CLASS (THIS REPORT)</p> <p>UNCLASSIFIED</p>	<p>21. NO. OF PAGES</p> <p>49</p>	<p>20. SECURITY CLASS (THIS PAGE)</p> <p>UNCLASSIFIED</p>	<p>22. Price</p> <p>\$4.50</p>